20

Radiation Effects on the Surfaces of the Galilean Satellites

R. E. Johnson
University of Virginia

R. W. Carlson
Jet Propulsion Laboratory, California Institute of Technology

J. F. Cooper
Raytheon Technical Services Company and NASA Goddard Space Flight Center

C. Paranicas
The Johns Hopkins University Applied Physics Laboratory

M. H. Moore
NASA Goddard Space Flight Center

M. C. Wong
Jet Propulsion Laboratory, California Institute of Technology

20.1 INTRODUCTION

The surfaces of Jupiter's moons are profoundly weathered by jovian charged particle and solar ultraviolet (UV) irradiation. Although early observations of the Galilean satellites suggested that their reflectance spectra were modified by energetic particles, it has only recently been shown quantitatively that radiolysis and photolysis, the chemical alteration of a surface by charge-particles and by the solar UV, are in fact occurring on the surfaces of these moons.

The irradiation of natural surfaces is one of a number of space weathering processes (Clark and Johnson 1996). It can produce new species in the surface, it can produce and eject volatiles into the atmosphere, and it can be a source of the local plasma (Figure 20.1 and Johnson 1990, 1996, 1998). There is extensive literature and current research on the radiation-induced weathering of the surface of the Earth's moon by solar wind ions. Although the lunar surface is refractory and the solar particle dose rate is modest, the effects of the incident radiation are evident as seen in the darkening of the surface (Hapke 2001). In contrast, Jupiter's large moons have frozen volatiles on their surfaces and are exposed to a much larger energetic particle flux. For example, the dose rate at Europa's surface is about 10^2 to 10^3 times the solar wind dose rate at the lunar surface. Therefore, the chemical changes made by the radiation are more pronounced and they determine many of the properties of the surfaces and atmospheres of the Galilean satellites.

Being able to describe the weathering of these surfaces is necessary to understand their atmospheres and to extract information on their composition and evolution. A key issue is determining if their reflectance spectra are representative of the intrinsic materials that may have been radiolytically altered or are representative of a patina of absorbing mate-

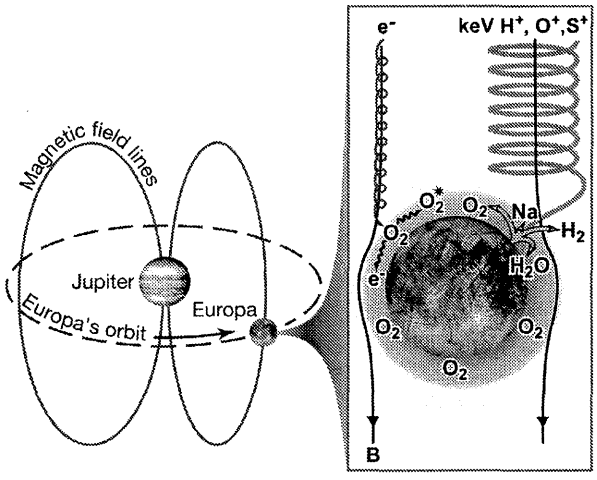

Figure 20.1. Sketch illustrating radiolysis processes of Europa's surface. Left: arrow indicates Europa's orbital motion, rotation of Jupiter's field and mean plasma flow leading to preferential irradiation of the trailing hemisphere. Right: Europa's trailing hemisphere and the "cork screw" motion of the energetic particles along deflected magnetic field lines. The roughly circular motion perpendicular to the field lines is the gyromotion, exaggerated here for electrons. Energetic ions and electrons produce electrolysis and sputtering of the surface, as discussed here, and low energy electrons and UV photons ionize the gas phase species as discussed in Chapter 19.

rial "painted on" by the energetic jovian particles and meteoroids. At Europa, it is also important to know whether there is a relationship between the putative subsurface ocean (Carr *et al.* 1998) and the composition of the surface and the atmosphere (e.g., Johnson *et al.* 1998, Kargel *et al.* 2000). The presence of an ocean is suggested by *Galileo* images (Chapter 15) and by magnetometer measurements (Chapter 21), but its chemical content is unknown. The presence of hydrated salt minerals, perhaps from brine formed from ocean salts, on a terrain fractured by tidal stress has been suggested to account for two bands in the *Galileo* Near Infrared Mapping Spectrometer (NIMS) spectra (McCord *et al.* 1998a, 1999, 2001a) and is consistent with satellite models that include upwelling of ocean material (e.g., Kargel *et al.* 2000, Zolotov and Shock 2001). However, alternate geochemical (McKinnon 2002; McKinnon and Zolensky 2003) and spectral (Carlson *et al.* 1999b, Dalton and Clark 1999, Dalton 2000, Carlson *et al.* 2003b) interpretations have been proposed. In this chapter we focus on the alteration of proposed surface materials by the incident radiation, with emphasis on the icy satellites, particularly Europa.

Europa is tidally heated like the inner, volcanic satellite Io, which may be an evolved, dehydrated version of Europa (Kargel *et al.* 2000). Ganymede and Callisto, on the other hand, appear to be less evolved. Although there is considerable disagreement, cratering studies suggest average geologic ages of the surfaces are of the order of 10^7 years for Europa, 5×10^8 years for Ganymede and 4×10^9 years for Callisto (Zahnle *et al.* 1998). Impact cratering affects these surfaces at kilometer depths, whereas regolith formation by meteoroid impacts can affect the surface to depths of tens of meters (Cooper *et al.* 2001). At equatorial and mid-latitudes, Io's surface is replaced by volcanism in times of the order of a year (Chapter 14). On the icy satellite surfaces the situation is less clear. Rising diapirs (plumes of warm, lower density ice) (Head and Pappalardo 1999) or water volcanism (Stevenson 1982, Squyers *et al.* 1983) may produce the mottled terrain covering much of Europa's surface on timescales as short as 10^4 years (Chapter 15). It has been suggested that liquid water may have flowed on to Ganymede's surface (Chapter 16), and Callisto's heavy cratered surface shows significant degradation (Chapter 17).

Radiolysis can alter the optical surface on relatively short timescales and produces chemical changes at micron to meter depths in times of $\sim$10 to 10^9 years respectively (Cooper *et al.* 2001, Paranicas *et al.* 2001, 2002). Radiolysis and photolysis compete with downward mixing by meteorite gardening, sublimation and burial, and subduction (Chapter 15), so that chemically-altered material can in principal be trapped at depths much greater than the radiation penetration depth. Hence, the oxygenated species formed by radiolysis and photolysis might act as an energy source for possible subsurface biological activity (Reynolds *et al.* 1983, Chyba 2000, Cooper *et al.* 2001, Chyba and Hand 2001, Chyba and Phillips 2001).

In order to infer the intrinsic components and geologic timescales, it is important to understand the weathering processes. Therefore, we bring together laboratory data on irradiation processing of ices and data on the jovian plasma needed to describe the effects of radiolysis on the jovian satellites. We first review those early observations of the Galilean satellites that indicated the potential importance of plasma bombardment. We then describe the radiation environment of these moons. This is followed by a brief review of the effect of the plasma on relevant surface materials. Finally, we summarize our present understanding of the radiation effects on each of the Galilean satellites and on the small inner moons.

20.2 EARLY OBSERVATIONS AND RESULTS

Since the Galilean satellites are most easily observed at eastern and western elongation, hemispheric reflectance differences between the leading and trailing hemispheres (in the sense of orbital motion) were noted over 30 years ago (e.g., Morrison 1982, Burns and Matthews 1986). Because *Pioneer* data (e.g., Simpson *et al.* 1974) indicated the presence of energetic particles that would strike the hemispheres asymmetrically, these hemispheric differences were attributed to Jupiter's trapped particle radiation. Satellite interactions with magnetospheric particles were also suggested by *Pioneer* data that showed "bite outs" in particle densities at the jovicentric orbits of some satellites, indicating absorption of energetic particles by these satellites (Mogro-Campero 1976). In addition, Ganymede and Io were observed to have subtle latitudinal variations in reflectance with some significant contrasts between equatorial and polar cap regions (Morrison 1982, Burns and Matthews 1986). These variations, initially thought to be due to thermal transport (Purves and Pilcher 1980, Sieveka and Johnson 1982) have subsequently been attributed to plasma bombardment (Johnson 1985, 1997).

The observation, prior to the arrival of the *Voyager* spacecraft, of a neutral sodium (Na) cloud emanating from Io (Brown and Chaffee 1974, Chapter 23), further stimulated interest in the plasma bombardment. Matson *et al.* (1974) suggested that sputtering by the jovian trapped plasma could produce the observed Na, and the laboratory work of Nash and Fanale (1977) described the effect of the incident plasma on possible surface constituents.

Since telescopic observations indicated that Europa, Ganymede and Callisto had cold, predominantly icy surfaces and since they are embedded in a plasma, Lanzerotti, Brown and co-workers (e.g., Lanzerotti *et al.* 1978) initiated a series of experiments to measure the effect of energetic charged particle irradiation on low-temperature ices. In doing so they discovered a new, robust process for ejection of molecules from frozen molecular solids, a process they called electronic sputtering (Brown *et al.* 1978). This is now understood to be a surface manifestation of radiolysis (Johnson 1990, 1996, 2001), the breaking of chemical bonds by energetic particles resulting in the formation of new molecular species and the release of energy. Based on their first set of measurements they estimated that kilometers of material may have been ejected from the surface of Europa over geologic timescales (Lanzerotti *et al.* 1978). This estimate was later reduced considerably, as discussed below. They also showed that the decomposition of water ice by the energetic ions would produce a thin O_2 atmosphere at Europa (Johnson *et al.* 1982). These suggestions generated considerable interest in radiation effects in ices. This interest has persisted, not only because of its relevance to the outer solar system bodies embedded in hot plasmas, but also because of

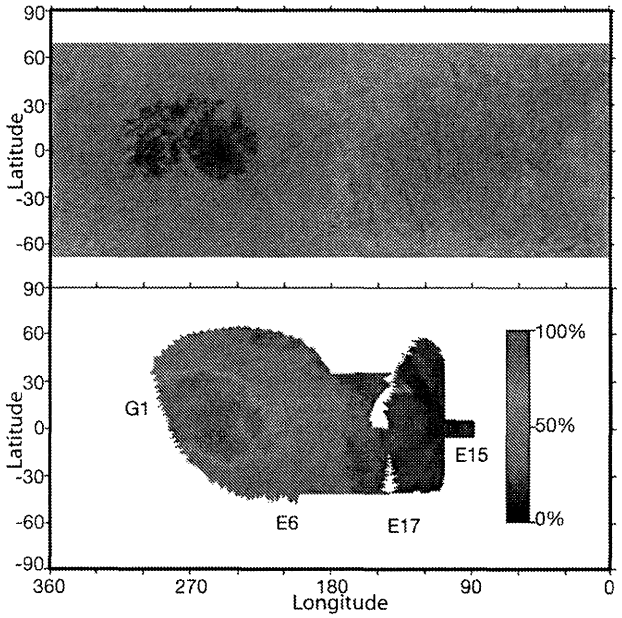

Figure 20.2. Compositional maps of Europa showing trailing hemisphere "bull's-eyes". (Above) *Voyager* ultraviolet (UV, 0.35 μm) to violet (VI, 0.41 μm) ratio map of Europa from McEwen (1986). Dark (blue) denotes more UV absorption relative to violet (VI). The trailing side enhancement was attributed to exogenic material such as sulfur implanted from the magnetosphere (McEwen 1986) or radiolytic processing producing sulfur (Johnson *et al.* 1988). (Below) Global distribution of Europa's hydrated material (Carlson *et al.* 2001, Carlson *et al.* 2003b) obtained by the *Galileo* NIMS experiment. Because the abundance of this hydrate correlates with the ultraviolet absorption pattern shown above, they are suggestive of radiolytic processing of a hydrated sulfur compound as discussed in the text (e.g., Carlson *et al.* 1999b). Bull's-eye patterns are also found on Ganymede and Callisto (see text). Such patterns may be produced by asymmetries in the fluxes of both electrons and ions and corresponding radiolysis and implantation effects. At the time of going to press a colour version of this figure was available for download from http://www.cambridge.org/9780521035453.

its relevance to the formation of pre-solar materials frozen on grains in the interstellar medium (e.g., Bernstein *et al.* 1995, Strazzulla 1998, Gerakines *et al.* 2000, 2001).

The longitudinal variations in reflectance measured by *Voyager* enhanced the case for exogenic modification of the surfaces of the icy satellites. For instance, McEwen (1986) suggested that the ultraviolet (UV, 0.35 μm) to violet (VI, 0.41 μm) ratio map (Figure 20.2a) indicates an exogenic component. In addition, the ratio of the reflectance in the UV filter to that in the orange (OR, 0.59 μm) filter data *vs.* Europa longitude correlated closely with the energetic particle flux to the surface, and the spectral slope in region ~0.3–0.5 μm suggested that sulfur was a principal contaminant at Europa (Johnson *et al.* 1988). The observation by Lane *et al.* (1981) of a UV absorption band, which they associated with SO_2 trapped in ice, was thought to be due to implantation of sulfur. In the last decade, new telescopic, Hubble Space Telescope (HST) and *Galileo* data have dramatically expanded our understanding of the role of radiolysis on the jovian satellites as described below.

20.3 CHARGED PARTICLE BOMBARDMENT

To quantify the effects of incident particle radiation, it is necessary to know the characteristics of the plasma environment and the nature of the interaction with the satellite. These determine the global bombardment pattern and the radiation dose as a function of depth at each location. For each impacting particle, this dose–depth relationship depends on species, energy, angle of incidence, and surface properties. At Jupiter, the plasma nearly corotates with the planet, continually overtaking the Galilean satellites in their orbital motion (illustrated in Figure 20.1). Therefore, cold plasma ions and electrons, which form the bulk of the plasma, flow preferentially on to the hemisphere trailing the satellite's motion. The lower density but higher energy particles bombard the satellite in more complex ways since the instantaneous velocity of an energetic particle can be quite different from the flow velocity. As is conventional when describing the jovian plasma, we will refer to ions and electrons below about 10 keV as "plasma" and above that energy as "energetic" particles.

Impacting particles exhibit spatial bombardment distributions across a satellite's surface that depend on their energy, mass, and charge, and on the influence of the electric and magnetic fields near the moon. These patterns can resemble the spatial distributions seen in reflectance in Figure 20.2 (e.g., Paranicas *et al.* 2001). The plasma flow, accounting for the effect of the satellite fields, has been described for a number of cases (e.g., Neubauer 1998, Liu *et al.* 2000). Here we consider an inert satellite embedded in the jovian magnetosphere which is a starting point for most models. By inert we mean that the electric and magnetic fields generated or induced in the satellite or its atmosphere/ionosphere are insignificant compared with fields in the ambient environment. When the intrinsic or induced fields associated with each moon are ignored, the spatial distribution of the bombardment is determined by the rate of flow of the plasma past the satellite and by the velocities of the plasma particles relative to the local magnetic field lines (Pospieszalska and Johnson 1989). The speed of the particles along the field lines determines the bounce time and the speed perpendicular to the field lines determines the gyroradius as indicated in Figure 20.1, r_g, the radius of gyration around the local magnetic field line. Particles can impact the leading hemisphere if their bounce times are comparable to or longer than the time for the plasma to flow past the satellite or if their gyroradius is comparable to or larger than the satellite radius.

The particle's gyroradius depends on its mass, speed, and charge and on the local magnetic field strength. The thermal plasma ions typically have gyroradii smaller than the satellite radius and preferentially impact the satellite's trailing hemisphere. However, energetic ions with significant velocities along the field line or with gyroradii comparable to the satellite dimensions can bombard the entire surface with an effective cross section larger than the satellite's physical cross section (Pospieszalska and Johnson 1989). The ratio of the gyroradius, r_g, to the satellite radius, R_s, is, $r_g/R_s = c(B)\,[(ME\sin^2\theta)^{1/2}/z]$, where E, M, and z are the ion's energy, mass and charge state, respectively, with θ the magnetic pitch angle (angle of the motion to the magnetic field line). For the average magnetic field B at the satellites,

Table 20.1. Satellite/plasma properties.

Satellite	Global Average Energy Flux (keV $(cm^{-2}\ s)^{-1}$)*	$c(B)$ **
Io	1×10^9 (1)	0.0014
Europa	5×10^{10} (2) 8×10^{10} (3)	0.0074
Ganymede	5×10^9 poles (3) 2×10^8 equator (3)	0.018
Callisto	2×10^8 (3)	0.19
UV(4)		
<280 nm (>4.4 eV)	4.0×10^{10}	
<207 nm (>6.0 eV)	7.6×10^8	

(1) Ions Mauk *et al.* (1996)
(2) (Ions and electrons >~10 keV) Figure 20.3
(3) (Ions and electrons >~10 keV) Cooper *et al.* 2001
(4) Globally averaged solar UV flux to each satellite as discussed by Cooper *et al.* (2001). Dissociation threshold for ice is ~6.0 eV (Orlando and Kimmel 1997)
* Uncertainties are ±50%
** $[r_g/R_s] = c(\mathrm{B})[(ME\ \sin^2\theta)^{1/2}/z]$. Value of c(B) for the average jovian field at satellite for charge state ($z = 1, 2, -$) and pitch angle θ, when ion's energy E is in keV and mass M is in am

values of c(B) are given in Table 20.1. At Europa, the gyroradius is equal to the moon's radius for 18 MeV protons, 1.1 MeV O^+ and 0.6 S^+ MeV when $\theta = 90°$. On the other hand the very energetic electrons, which have small gyroradii and travel rapidly along the magnetic field compared with the corotation speed of the plasma, principally bombard the equatorial, trailing hemisphere (Paranicas *et al.* 2001). Therefore, the common finding of "bulls-eye" patterns (e.g., Figure 20.2) centered on the trailing hemispheres for certain irradiation products, initially thought to be due to the plasma ion bombardment, could also be a result of radiolysis induced by the energetic electrons.

The electric and magnetic fields near the satellites can radically modify the particle flux to a satellite's surface. Ganymede's magnetosphere is a good example because recent data have shown that particle intensities are much different on "open" and "closed" field lines (Williams *et al.* 1998). This means that, to lowest order, the bombardment pattern is dictated by Ganymede's internal magnetic dipole, allowing more direct access at the poles than at the equator, as is the case at the Earth. Consequences are the production of an oxygen aurora near the poles (Hall *et al.* 1995, 1998) and, possibly, the observed "polar cap" (Johnson 1997, Chapter 16), as well as the deflection of energetic ions up to ~10 MeV and all energetic electrons from the equatorial region (Cooper *et al.* 2001). However, the low-energy plasma might be able to penetrate the equatorial region (Volwerk *et al.* 1999, Cooper *et al.* 2001) in the absence of strong ionospheric electric fields.

The net charged particle flux to each surface, assuming a magnetically inert satellite, except where noted, is given in Table 20.1 and is compared to the solar UV energy flux. In Figure 20.3 we also give the energy flux carried by the electrons and the principal ions (H^+, O^{+z} and S^{+z}) measured upstream from Europa. The energy is carried pri-

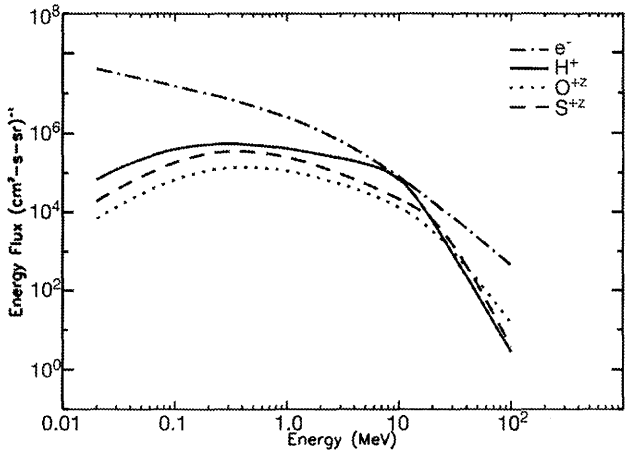

Figure 20.3. The differential energy flux upstream from Europa for energetic electrons (Paranicas *et al.* 2001) and H^+, O^{+z} and S^{+z} ions averaged from three spectra from 1997–2001 (Paranicas *et al.* 2002). To obtain the energy flux across a surface the pitch angle distribution is needed. For an approximately isotropic distribution multiply by π steradians. The integrated energy fluxes from 10 keV to 200 MeV in [keV $(cm^{-2}\ s)^{-1}$)] are: e^- (3.6×10^{10}), H^+ (7.3×10^9), O^{+z} (1.8×10^9), S^{+z} (3.4×10^9).

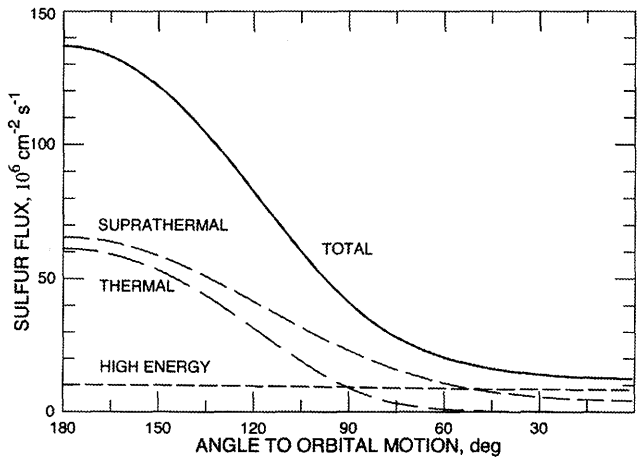

Figure 20.4. Angular distribution of sulfur implantation on Europa (Carlson *et al.* 2001, Carlson *et al.* 2003b). This estimate uses Bagenal's (1994) values for the iogenic plasma and assumes undeviated plasma flow on to an inert Europa. Note the trailing side enhancement. Asynchronous rotation and gardening would also influence the resulting surface density profile.

marily by energetic particles and not by the plasma (Mauk *et al.* 1996) and the energetic protons and electrons are the dominant carriers of energy (Cooper *et al.* 2001, Paranicas *et al.* 2001), contrary to earlier assumptions (Shi *et al.* 1995). Recent measurements of charged particle fluxes upstream of Europa indicate that the net energy flux to the trailing hemisphere due to the energetic electrons can be larger than that due to the ions (Paranicas *et al.* 2002). From Table 20.1 it is also seen that photolysis by the solar UV can be a significant contributor and at Callisto the energy deposited by those UV photons that are energetic enough to dissociate water ice is larger than the energetic particle energy flux.

The preferential bombardment of the trailing hemi-

sphere determines the spatial distribution of implanted, reactive species such as carbon and sulfur. Sulfur implantation rates are an order of magnitude higher on Europa's trailing hemisphere than at the apex of the leading hemisphere as seen in Figure 20.4 (Carlson 2001, Carlson *et al.* 2003b). Whereas the carbon ion abundance has not yet been quantified in the plasma, *Voyager* measurements in the ~1 MeV per nucleon range give C/S ~0.2 near Europa's orbit and ~1 near Callisto (Hamilton *et al.* 1981). At higher energies (4–18 MeV per nucleon), the C/S ratio increases from ~1 at Europa and ~5 at Ganymede to ~20 at Callisto (Cohen *et al.* 2001). A C/S ratio that increases with increasing energy suggests that the energetic carbon preferentially comes from the outer jovian magnetosphere and sulfur predominantly from the inner magnetosphere. Carbon ions in the solar wind can have easy access and undergo large gains in energy during inward diffusion (cf. Schulz 1979, Barbosa 1994) and Callisto's atmosphere can be a source of carbon. By contrast, sulfur ions reaching Callisto's orbit from the Io plasma torus are less accelerated. Neutralized sulfur ions emitted outward from the torus can be re-ionized in the outer magnetosphere and diffuse inward providing an energetic sulfur component (Eviatar and Barbosa 1984). These would have a lower charge state than the solar wind carbon ions that are fully stripped. Therefore, high charge state carbon ion implantation would tend to be concentrated on Callisto's trailing hemisphere.

The measurement of abundant oxygen and sulfur ions at keV to MeV energies has a significant effect on sputtering since the yields of the order of 10^3 per incident ion are expected at these energies (Johnson 1990, Shi *et al.* 1995). We give in Table 20.2 the globally averaged ice resurfacing rates due to sputtering for Europa, Ganymede's equatorial region and polar caps, and Callisto (Cooper *et al.* 2001). Lanzerotti *et al.* (1978) extrapolated *Pioneer* data and obtained an upper limit ~1 μm yr^{-1} (1 km Gyr^{-1}) at Europa. Johnson *et al.* (1981) and Shi *et al.* (1995) greatly reduced this limit but left open the possibility of high rates due to incident oxygen ions since the *Voyager* Low Energy Charged Particle (LECP) experiment only measured the total ion flux. The Energetic Particle Detector (EPD) on *Galileo* provided mass resolution (Ip *et al.* 1997, 1998, 2000, Paranicas *et al.* 1999, 2002, Cooper *et al.* 2001). This resulted in lower average yields as protons were found to dominate the flux. The rates are about an order of magnitude higher at Ganymede's polar caps than at its equator (Cooper *et al.* 2001), although the plasma ion input is uncertain and the cap region is much smaller. The composition of thermal plasma at the icy satellites remains uncertain, leading to differences in estimates (cf. Paranicas *et al.* 1999, Shi *et al.* 1995). Since the escape fractions for sputtered H_2O on the icy satellites are 20–30% (Johnson *et al.* 1983, Johnson 1990), most of the water molecules return to the surface. The cumulative sputtering rates can be competitive with the net sublimation rate (Johnson 1990), therefore a 3-D model which includes both sublimation and sputtering is needed.

20.3.1 Variability

Variations in fluxes of energetic particles have been measured by *Voyager* and *Galileo*, particularly in the Io torus. Energetic particle energy fluxes near the orbit of Io declined by a factor of five between the *Voyager* and *Galileo* epochs as compared by Mauk *et al.* (1998). Such changes have been attributed to the variability of neutral gas escaping from Io and its action, via charge exchange, on the ambient hot plasma. It is possible that the variations in the reflectance spectra seen on Ganymede and Europa (Domingue and Lane 1998a,b, Domingue *et al.* 1998) are due to changing abundances of radiolytically-produced ultraviolet absorbers caused by magnetospheric variability.

The intensity of magnetospheric particle irradiation also varies with the satellite's position within the jovian current sheet during Jupiter's 10-hour rotation. Paranicas *et al.* (2001) found an order-of-magnitude variation in >10 keV electron flux spectra for three *Galileo* flybys of Europa and the total energy flux upstream of Europa was about a factor of two less than on an earlier flyby reported by Cooper *et al.* (2001) (e.g., Table 20.1).

The jovian plasma environment is likely to have been very different thousands to billions of years ago than it is today due to orbit variations, early volcanic activity, and changes in the solar flux. In addition, changes in the internal conditions of the satellites could modify their interactions with the magnetosphere. Here we assume that computed irradiation parameters are valid to within about an order of magnitude. Since the present level of irradiation is sufficient for radiolytic processing of Europa's surface ices within tens of years at micron depths (Cooper *et al.* 2001), it may not matter in describing the reflectance that the intensities averaged over geologic times differ. However, the possibility of an earlier, more intense rate of implantation could be important when accounting, for instance, for the net sources of sulfur or sodium in Europa's crust.

20.4 DOSE *vs.* DEPTH

Incident ions and electrons lose their energy to atoms and molecules in the surface by a number of processes. It is this deposited energy that drives the chemistry described below. To first order, the energetic ions (> a few keV amu^{-1}) and the electrons primarily lose their energy to the solid by producing excitations and ionizations. Ions also lose energy by momentum transfer (knock-on) collisions with atoms in the solid. This becomes the dominant loss process at low energies (< a few keV amu^{-1}). Finally, scattering of very energetic electrons produces bremsstrahlung radiation at X-ray to gamma-ray energies, which also leads to ionizations and secondary electrons. The total energy loss per unit path length in the solid, called the *stopping power*, is written as (dE/dx) (e.g., Johnson 1990), for which tables and computer codes are available. Integrating over the energy loss and accounting for deflections, the penetration depth into the material is determined. This is called the *projected range* and depends on particle type and energy. The heavy ions, which interact strongly with the solid, have the smallest penetration depth and the fast protons and electrons the largest. For example, 10 keV S^+, H^+ and electrons penetrate ice to depth of ~0.03, 0.3, 10 μm respectively (e.g., Johnson 1990).

Estimates of the dose (energy per unit volume) *vs.* depth can be obtained from the stopping power. However, to obtain accurate values of dose *vs.* depth, account must be taken of the transport and energy deposition of the secondaries

Table 20.2. Resurfacing rates for the icy Galilean satellites [μm yr^{-1} = 10^{11} mol. (cm^{-2} s)$^{-1}$].

Reference	Process	Europa	Ganymede	Callisto
Lanzerotti *et al.* (1978)	H^+	0.005–1.3	0.0005–0.13	0.000 01–0.003
Johnson *et al.* (1981)	H^+	0.0009	0.0006	0.000 05
Johnson *et al.* (1981)	O^+	0.094	0.057	0.005
Shi *et al.* (1995)	O^+	0.35	0.19	0.019
Ip *et al.* (1997)	H^+, O^+, S^+		0.004–0.017	
Ip *et al.* (1998)	H^+, O^+, S^+	0.80		
Paranicas *et al.* (1999)	H^+, O^+, S^+		0.008	
Krüger *et al.* (2000)	Meteoroid		0.34	
Ip *et al.* (2000)	H^+, O^+, S^+	0.056–0.56		
Cooper *et al.* (2001)	H^+, O^+, S^+	0.016	0.004 polar 8×10^{-4} equator	0.0004
Cooper *et al.* (2001)	Sublimation	0.000 07 (106 K)	0.16 (124 K)	0.004 (115 K)
Cooper *et al.* (2001)	Meteoroid	1.2	1.2	1.2
Paranicas *et al.* 2002	H^+, O^+, S^+	0.08		

Sputtering yields do not include enhancements due to temperature, incident angle and decomposition (Johnson 1990). For comparison we removed factor of 1/4 for global averaging from trailing hemisphere bombardment by an approximately unidirectional corotating plasma from sputtering rates of Shi *et al.* (1995) and the factor 1 to 4 for porosity of the target is set to unity. Low and high values from the Ip *et al.* (1998, 2000) are, respectively, without and with secondary sputtering by pickup ions.

produced. That is, knock-on collisions set fast atoms in motion, ionizations produce fast electrons, and the excitations and bremsstrahlung yield photons. These redistribute the deposited energy. The radiation dose *vs.* depth for Europa, Ganymede and Callisto has been calculated using *Galileo* data for the particle energy spectra (Cooper *et al.* 2001). For all three satellites, computed energetic particle doses at depths up to a few microns are dominated by ions and at depths greater than 10 microns by electrons. The immediate surface layer (~0.01 μm) is modified by those corotating thermal plasma ions that reach the satellite surface. The flux of low-energy electrons to the surface is not known but would also contribute in this layer. At Europa, the dose at meter depths on the trailing hemisphere is dominated by bremsstrahlung gamma-rays produced by the >10 MeV electrons (Paranicas *et al.* 2002). Due to the variations described above, Paranicas *et al.* (2002) find a 1–2 orders of magnitude higher dose beyond millimeter depths below the surface of Europa than does Cooper *et al.* (2001). Figure 20.5 gives the time in years at each depth to accumulate a dose of ~100 eV per 16 amu (mass of O). In standard dosage units this about 60 gigarads at Europa, sufficient to ionize every water molecule ~4 times.

The dose *vs.* depth also exhibits spatial variations, because the relative fluxes of particles with different penetration depths vary over the surface. The leading/trailing differences in dose at depth, discussed above, are larger than the differences in total energy flux to the surface. For instance, at 0.1 mm the total dose rate due to energetic charged particles will be a factor of ~1000 smaller on the leading hemisphere and in the polar regions, than in the equatorial region of Europa's trailing hemisphere (Paranicas *et al.* 2002). The differences with depth can be important in modeling reflectance spectra, since the photons sample very different depths depending on the absorption and scattering properties of the regolith at the photon's wavelength. Typical sampling depths range from the grain size (tens to hundreds of μm) to about a mm (e.g., Geissler *et al.* 2000, Hansen and McCord 2004). For highly absorbing material, surface Fresnel reflection samples about a wavelength into the medium.

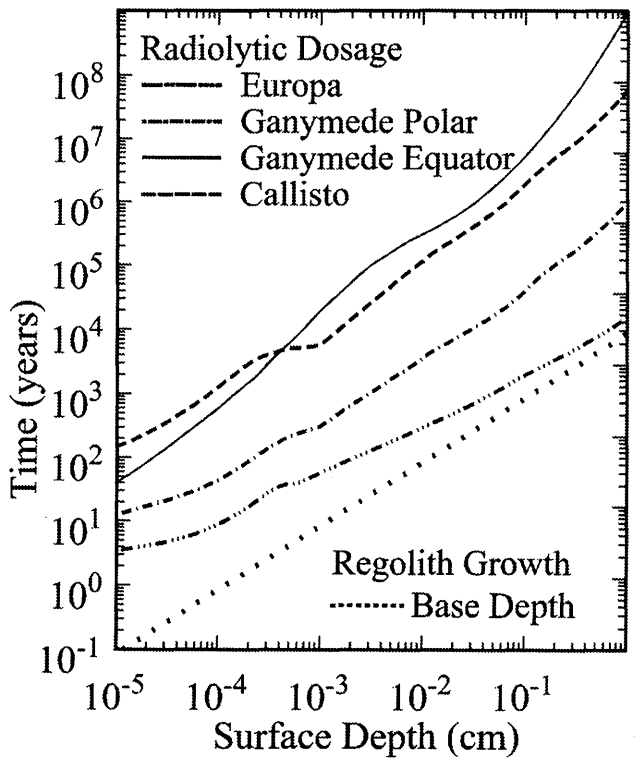

Figure 20.5. Time *vs.* depth for accumulating a significant dose, 100 eV (16u)$^{-1}$ (Cooper *et al.* 2001), compared to the time for the regolith to grow to that depth. The radiolytic time can be scaled by a G-value ($t_x = t/G_x$) to give the time to form a product molecule, x, per 16u of material.

20.4.1 Radiation and Regolith Formation

Because of the rapid resurfacing by volcanism and sublimation/condensation, micrometeoroid impacts play a negligible role at Io. However, on the icy Galilean satellites and the small inner satellites, regolith formation by interplanetary meteoroid impact is important. In contrast to the plasma, meteoroids predominantly bombard the hemispheres leading the satellite's motion. Therefore, peaks in the spatial distribution of meteoroid and plasma bombardment are expected to occur at opposite longitudes.

Because of gravitational focusing by Jupiter, the meteoroid flux and impact velocity increase by a factor of two to three within the realm of the Galilean satellites. These impacts fracture, excavate, and redistribute the icy surface material, producing a porous regolith. The ice grains are also sintered by the impacts affecting the thermal conductivity (Grundy *et al.* 2001) which may vary considerably across the surface (Spencer *et al.* 1999). Estimated regolith growth rates differ mainly in the ejecta yield per incident mass flux (e.g., Cooper *et al.* 2001, Krüger *et al.* 2000). The globally averaged flux is $\sim$1.4–1.5 $\times$ 10^{-16} g cm^{-2} s^{-1} for the icy Galilean satellites which are preferentially bombarded on their leading hemispheres. Accounting for the satellites' diameter and gravity, $\sim$45 g s^{-1}, $\sim$130 g s^{-1} and $\sim$110 g s^{-1} are delivered to Europa, Ganymede and Callisto respectively by meteoroids with typical size $\sim$100 μm and mass $\sim 10^{-5}$ g. For most meteoroid types the sulfur mass abundance is $\sim$6 %, whereas the carbon abundance varies from 3.4% for the CI chondrites to 24% for organic comet dust (CHON particles; Li 2000). These provide 3, 8, and 7 g s^{-1} of sulfur to Europa, Ganymede, and Callisto respectively and 0.5–4 times more carbon. Table 20.3 summarizes the source strengths for sulfur and sodium at Europa and indicates that the ion implantation rates dominate the meteoroid supply rate for these atoms.

Meteoroid impacts primarily convert their incident mass and energy ($\sim$20 km s^{-1}) into orders of magnitude more ejecta. Resurfacing rates for ion sputtering, meteoroid impact, and sublimation in Table 20.2 indicate that meteoroid bombardment and sublimation dominate sputtering. Meteoroid erosion rates $\sim$0.3–1.2 μm per year are roughly consistent with erosion rates for Ganymede's crater rays: $\sim$20 m Gyr^{-1} at the leading apex and $\sim$1 m Gyr^{-1} at the trailing apex (Shoemaker *et al.* 1982). Regolith depths of $\sim$tens of meters on Callisto are consistent with observations of smooth dark material burying the remains of small craters. But this could also be due to sublimation-driven (CO_2) degradation of crater structures (Moore *et al.* 1999). Deepening of the regolith to meter depths after 10^5 years is assumed to be proportional to $t^{1/2}$, as in lunar studies (Morris 1978), since all new impacts must first penetrate the accumulated regolith (Cooper *et al.* 2001). In Figure 20.5, the times for accumulating a significant dose are compared to the much shorter, *globally averaged* times for the regolith growth to a given depth.

Although only the top millimeter of the regolith is accessible to remote sensing, radiolysis indirectly affects the properties of the regolith at much greater depths. That is, the chemistry induced at depth is determined by the particle penetration discussed above and by the meteoroid mixing of products downward. Impact gardening will reduce the accumulated dose by burial and will expose material brought from below. Because of the continual overturning of the regolith, much of the newly exposed material would have been exposed earlier. Therefore, the cumulative dose in a volume of material can exceed that absorbed in the burial time. The total dose depends on the radiolysis and gardening rates. Both are spatially variable, with the radiolysis rate being greater on the trailing hemisphere while the gardening rate is greater on the leading hemisphere. This enhances the leading–trailing asymmetry in chemical products. This asymmetry is reduced if there is asynchronous rotation of the crust, as discussed in the Europa section below.

The surface created by meteoroid bombardment is a porous regolith consisting of a relatively small mass fraction of grains that have been flash heated and even vaporized by impacts and a much larger mass fraction of thermally unprocessed grains that have been displaced as ejecta from impact sites to surrounding areas. Grain sizes of the order of $\sim$50–500 μm have been suggested. The porosity can significantly lower the sputtering yields (Johnson 1989) and very small grains are sputtered more efficiently by energetic ions (Jurac *et al.* 2001). The granular nature can also affect material transport. That is, although some subsurface material appears to act as an electrical conductor, affecting the magnetic signature of the icy satellites (Kivelson *et al.* 1999), their surfaces are primarily electrical insulators. Therefore, they charge readily under irradiation (Jurac *et al.* 1995). This has only a minor effect on the flow of charge to the surface, but electrostatic levitation and transport of grains can occur due to the charging if the grains are not sintered. This was shown to occur efficiently at the lunar terminators, but such processes have not yet been modeled for the Galilean satellites.

20.4.2 Trapping and Escape

Because the regolith grows, on the average, faster than radiolytic products accumulate (Figure 20.5), the satellite surfaces can be a substantial reservoir of buried radiation-altered material. The ability to trap a molecule depends on its size and the strength of its interaction with the matrix molecules. Refractory products, such as molecules having carbon and sulfur chains, are readily retained in the ice matrix, as are radiation products OH and H_2O_2, and species which become hydrated, such as NH_3 and CH_3OH.

Radiolytic reactions also produce volatile gas molecules (H_2, O_2, SO_2, CO_2, CO), as discussed below. Very volatile products, such as H_2, readily diffuse through the lattice and escape to space. Because H_2O is a polar molecule, some volatile products can be trapped in ice at temperatures well above their solid sublimation temperatures (e.g., Bar-Nun *et al.* 1985). Molecules typically trap at defects, in voids and at grain boundaries. The mobility through the lattice is determined by defect diffusion, which in ice occurs above $\sim$100 K (e.g., Johnson and Quickenden 1997). On becoming mobile, the defects accumulate to form voids, and trapped volatiles can segregate, forming inclusions in ice (Johnson and Jesser 1997). Voids can also form due to local concentrations of salts (e.g., brine channels and pores frequently found in terrestrial sea ice) lowering the local melting temperature. The low melting point of sulfuric acid hydrate ($\sim$220 K, Zelenik 1991) also promotes melt channels and

Table 20.3. Europa source and sinks [global average in atoms $(cm^2\ s)^{-1}$.

	Implantation	Micrometeorites	Io Neutrals *	Loss to Space
Na	$0.2–0.8 \times 10^6$	0.05×10^6	$\sim 4. \times 10^4$	$4–9 \times 10^6$
S	$0.2–1.4 \times 10^8$	$\sim 0.1 \times 10^6$	$\sim 1. \times 10^6$	$\sim 1 \times 10^7$

* Charge exchange in the Io torus produces a "wind" of energetic neutrals flowing out from Io [S value from (Cooper *et al.* 2001); Na $\sim 0.04 \times$ S]. Charged grains can also carry iogenic material to Europa.

void production. Because the ability to diffuse depends on the defect density, pore size and grain size, measuring trapping at conditions on the icy satellites is difficult. In laboratory ices formed by vapor deposition, O_2 is retained inefficiently at the temperatures like those on the icy satellites (Baragiola *et al.* 1999). However, observations suggest that radiolytically formed O_2 is trapped in icy satellite surfaces (e.g., Calvin *et al.* 1996, Cooper *et al.* 2003), although extremely cold shaded regions have been suggested (Baragiola and Bahr 1998).

Based on the above, a substantial reservoir of buried oxidants (H_2O_2, HO_2, O_2, SO_2, CO_2 etc.) might exist at Europa (Johnson *et al.* 2003). These may eventually be subducted into the putative subsurface ocean (Cooper *et al.* 2001). On the other hand, those volatile products that escape from depth by diffusion (Livingston *et al.* 2002) or percolation through the radiation-damaged regolith contribute to the satellite's atmosphere. Therefore, the total energy flux in Table 20.1 scaled by the radiolytic yield of volatiles can be used to give an upper bound to the atmospheric source rate and the net surface erosion rate. This rate, unlike the sputtering rates in Table 20.2, can exceed the meteoroid impact erosion rate. Such a devolatilization process would peak at the apex (the "bull's-eye") of the trailing hemisphere leading to a concentration of non-volatile, non-ice species.

20.5 RADIATION EFFECTS

The energy deposited by incident ions, electrons or photons alters the surface chemically (radiolysis) and physically by the production of damage (amorphization) and by the ejection of atoms and molecules (sputtering or desorption). The fast ions and electrons, which dominate the energy flux to the surfaces of the Galilean satellites, produce ionization tracks with the average energy deposited per ionization event called the W-value. On recombination, energy is released affecting the local lattice structure and radicals are produced, often by dissociative recombination. The production of a density of mobile and trapped radicals can lead to chemical reactions. Since the dissociated products immediately collide with neighbors (cage effect), reactions back to the initial molecule are enhanced in a solid. Chemical formation of new species is favored in regions of high excitation density ($\sim$2 nm) called spurs (Spinks and Woods 1990). For instance, a 1 MeV proton in ice ($W \sim 20$ eV), produces on the average $\sim 5 \times 10^4$ ionizations, and $\sim 10^4$ spurs each containing a number of ionizations.

The word sputtering typically applies to ejection of surface material by knock-on collisions. However, the dissociations and chemical reactions produced by ionizing radiation also releases energy to the lattice. In low-cohesive-energy materials, like the low-temperature frozen volatiles in the outer solar system, this energy can cause the ejection of atoms or molecules and can produce defects. Therefore, radiation damage, sputtering and radiolysis are closely related. Although there are a number of review articles on these processes (e.g., Strazzulla 1998, Johnson 1996, 1998, Madey *et al.* 2002, Baragiola 2003, Johnson *et al.* 2003), there are still very large gaps in our understanding for the materials and temperatures of interest for the Galilean satellites.

Results for defect formation, sputtering and radiolysis are typically given as yields. The sputtering yield is the number of atoms or molecules ejected per incident particle. For radiolysis, the yield is given as a G-value, the number of molecules formed per 100 eV of energy deposited or as the energy per target molecule deposited for a given effect (eV per molecule). These can be combined with the energy deposition, as in Table 20.1, to give a product yield. G-values vary considerably as they depend on the energy density deposited and, hence, on the particle type and energy. Therefore, lightly ionizing radiations, such MeV protons, keV electrons and UV photons can have G-values very different from those for keV oxygen and sulfur ions. G-values also depend on surface temperature and on radiation dose. At high doses, back reactions can destroy the primary products, giving a dose-independent plateau in the concentration of primary products. Therefore, large numbers of measurements are needed, or models are needed that describe electron transport and use absolute cross-section measurements (e.g., Sieger *et al.* 1998, Gomis *et al.* 2004). We first summarize the results for ice, a principal surface constituent on three of the satellites, and then consider species containing sulfur, carbon and alkalis, which comprise the bulk of the material confirmed by reflectance spectra. We omit nitrogen-containing species since they have yet to be clearly identified on the jovian satellites.

20.5.1 Irradiation of Ice

In Figure 20.6 is given a summary of the measured sputtering yields at temperatures $\leq$80–100 K where the dominant ejecta is H_2O. These are presented as yields *vs.* incident ion velocity with both variables scaled by the nuclear charge of the ion with the fitting parameters given in the caption. The scaling used fails at the lowest energies where knock-on collisions dominate, but is useful over the range of energies of interest at the icy Galilean satellites (Figure 20.3). At higher surface temperatures, the yield becomes temperature dependent and the ejection of H_2 and O_2 become important (Reimann *et al.* 1984, Baragiola *et al.* 2003, Johnson *et al.* 2003).

Following electronic excitations and ionizations water molecules are dissociated and the irradiated ice is gradually altered (Reimann *et al.* 1984, Benit *et al.* 1987) with the

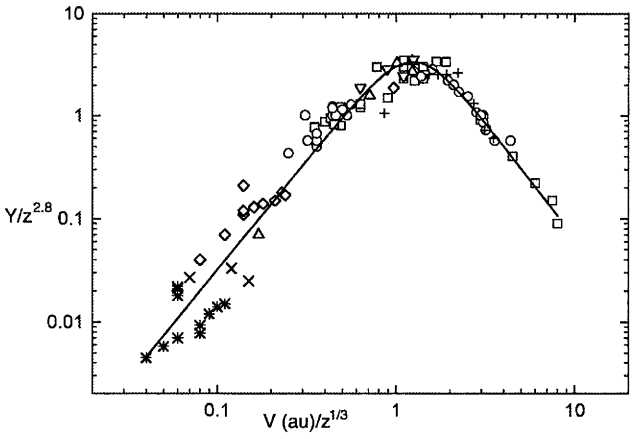

Figure 20.6. Sputtering yield, Y, *vs.* incident ion velocity, v, for water ice <100 K. The yield is given in terms of net H_2O ejected. Both the velocity and the yield are scaled by the nuclear charge, Z, of the incident ion. The points are the accumulated data for a number of incident ions. The line is a rough fit given by $Y^{-1} = Y_H^{-1} + Y_L^{-1}$ with $Y_H/Z^{2.8} = 11.2\ (v/Z^{1/3})^{-2.24}$ and $Y_L/Z^{2.8} = 4.2\ (v/Z^{1/3})^{2.16}$. The fit is poor for very low-velocity ions where elastic nuclear energy loss is dominant. Velocity is given in atomic units (1 au = 2.18×10^8 cm s^{-1}). (See www.people.virginia.edu/~rej for data at other temperatures and for other ices).

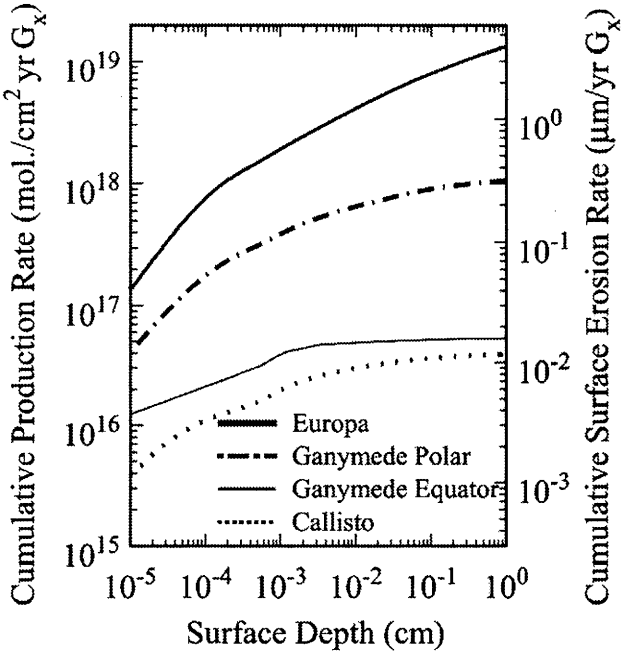

Figure 20.7. Cumulative production rate in molecules per unit time and surface area for radiolytic product x with yield G_x on surface regions of the icy Galilean satellites. The right axis shows the approximate associated local erosion rate for H_2O ice under the assumption that one H_2O molecule is removed for each product molecule. When using the G-value for O_2, two water molecules are removed so the erosion rate is twice that indicated.

density of trapped product species reaching a steady state. The principal dissociation product is H + OH with a much smaller fraction of H_2 + O, possibly only occurring at surfaces, grain boundaries and voids (Watanabe *et al.* 2000). At the temperatures on the icy satellites, H diffuses readily until it reacts, whereas the OH and O trap. Trapped OH has been seen in the UV in laboratory measurements (cf. Taub and Eiben 1968, Johnson and Quickenden 1997). In addition, OH–H_2O (Langford *et al.* 2000) and O–H_2O (Khriachtchev *et al.* 1997) have been studied by matrix isolation techniques. Trapped OH absorbs at about 0.28 μm, but has not yet been clearly identified on these satellites (Johnson and Quickenden 1997). It was suggested to be a component of Ganymede's UV band associated with O_3 at 0.26 μm (Noll *et al.* 1996) and overlaps Europa's band associated with SO_2 at about 0.28 μm (Lane *et al.* 1981, Noll *et al.* 1995). However, the steady state concentration may be too low to observe at the relevant temperatures, since OH can diffuse above about 80–100 K. On increasing temperature the above radicals are mobilized (Matich *et al.* 1993) possibly producing oxygen via (O + OH → O_2 + H). Mobilization also produces reactions back to H_2O (OH + OH → H_2O + O) and additional new molecules (Kimmel *et al.* 1994, Orlando and Kimmel 1997) such as H_2O_2 and HO_2. Trapped H_2O_2, present on Europa (Carlson *et al.* 1999a), is seen in MeV proton-irradiated ice only at low temperatures (Moore and Hudson 2000), but is apparently more readily produced by lower energy protons and heavy ions (Gomis *et al.* 2004). Therefore, it is likely formed from closely spaced OH in a spur or by production of O–H_2O and a rearrangement (Khriachtchev *et al.* 2000). Finally, charged species (positive ions by direct ionization and negative ions by attachment of secondary electrons) can affect the chemical pathways (cf. Kimmel *et al.* 1994).

Molecular hydrogen, (H_2), is formed directly, as indicated above, and by H + H → H_2 and H + OH → O + H_2 reactions as well as reactions involving charged species (Kimmel and Orlando 1995). Since H_2 readily diffuses at the relevant temperatures, it escapes from the ice so that the surface becomes oxidizing (Johnson and Quickenden 1997). On further irradiation O_2 can form and escape retaining the near stochiometry of the ice (Reimann *et al.* 1984). This may occur by reactions of trapped O with either O or OH (Matich *et al.* 1993) or by excitation of a precursor species such as H_2O_2 or HO_2 (Sieger *et al.* 1998) or trapped O (Matich *et al.* 1993, Johnson *et al.* 2003). The O might trap in a substitution or interstitial site or as O–H_2O, a molecule seen in matrix isolation studies (Khriachtchev *et al.* 1997). Recently, individual peroxide molecules were shown not to be likely precursors in pure ice (Johnson *et al.* 2003), but in ice under long-term irradiation trapped oxygen molecules may form readily in peroxide inclusions in ice (Cooper *et al.* 2003), suggesting a possible spatial relation between trapped oxygen and peroxide.

Ozone, O_3, apparently seen in reflectance on the icy satellites (e.g., Noll *et al.* 1996), is not seen as a radiation product in pure ice (Gerakines *et al.* 1996, Bahr *et al.* 2001). This is likely due to the efficient diffusion of H and its reaction with O_2 and its precursors. The formation and stability of O_3 and H_2O_2 can be enhanced by the presence of an additional oxidant. At satellite surface temperatures, peroxide destruction by secondary electrons is apparently

reduced by the presence of electron scavengers such as O_2 and CO_2 (Moore and Hudson 2000). The latter is a likely contaminant in the early experiments possibly causing the high measured *G*-values (cf. Hart and Platzman 1961) and is also known to be present on the icy Galilean satellites (Carlson *et al.* 1996, McCord *et al.* 1997, 1998a, Carlson 1999, 2001). Since O_3 readily forms in condensed O_2, the accumulation of oxygen in extremely low-temperature, shaded regions (Baragiola and Bahr 1998, Baragiola *et al.* 1999) or in voids (Johnson and Jesser 1997, Johnson 1999) is likely a prerequisite to O_3 formation. Because the UV bands in which H_2O_2 and O_3 have been observed also lead to dissociation, chemical change by photolysis is also occurring on these surfaces. Finally, O_2 and O_3 can be produced in other suggested surface materials. For instance, under irradiation silicates lose oxygen, probably as O_2 (Walters *et al.* 1988), and recently O_3 has been seen as an interstitial molecule in glassy SiO_2 (Skuja *et al.* 2000). O_2 is also a radiation product of sulfates and carbonates.

In laboratory experiments the dissociation products, H, H_2 and O, have been seen as excited ejecta from the surface layer (Kimmel and Orlando 1995). If the yields and the sample temperatures are both low, radicals (e.g., H, O) ejected from the surface layer can be important. However, energetic heavy ions produce large yields of the order of 10–1000 molecules per ion and the principal ejecta are those species with the lowest binding energy to the solid: H_2O and its volatile decomposition products H_2 and O_2 (e.g., Johnson 1990). Whereas the yield of H_2O is nearly independent of temperature and dose, the yields of H_2 and O_2 are not (Brown *et al.* 1982, Sieger *et al.* 1998). H_2 is ejected promptly, as discussed, but also exhibits a dose-dependent component. The prompt ejection permanently changes the ice chemistry, allowing the formation and loss of O_2 (e.g., Johnson *et al.* 2003). Therefore, the O_2 sputtering yield depends on both temperature and dose. Its formation and loss control the dose-dependent component of the H_2 yield (Reimann *et al.* 1984).

At average temperatures relevant to the icy satellites (~100 K) ejecta mass ratios of O_2 to H_2O of about 0.1–0.2 are expected, based on energetic ion sputtering measurements (e.g., Brown *et al.* 1984). Such ratios have been used in a number of modeling studies, however, larger ratios are expected for a number of reasons. Low-energy ions may produce chemical change more efficiently (Bar-Nun *et al.* 1985, Baragiola *et al.* 2003) and at the highest relevant surface temperatures (>120 K) O_2 can become the dominant ejecta (Brown *et al.* 1982, Sieger *et al.* 1998). In addition, sputtering occurs from a porous regolith in which ejected H_2O molecules stick efficiently on neighboring grains (Stirniman *et al.* 1996, Smith and Kay 1997) but O_2 will not. The sticking of H_2O reduces its effective yield (~1/4, Johnson 1989) enhancing the relative importance of O_2. Finally, the radiation can cause the O_2 and other volatiles produced at depth in a solid to diffuse to the surface and escape (Benit and Brown 1990).

The sputtering and production of volatiles is typically also accompanied by radiation damage to crystalline ice. At low temperatures this efficiently produces amorphous regions (Leto and Baratta 2003) and defects that can aggregate and act as scattering centers modifying the "effective grain size." This effect has apparently been seen in reflectance on the Galilean satellites (Hillier *et al.* 1996, Hansen and McCord 2004). It has been suggested to lead to surface brightening in cold regions (Johnson 1985, 1997), although this is very sensitive to the radiation penetration depth and sample temperature (e.g., Baragiola 2003).

The above discussion is for ice without impurities. It is important to remember that, even when H_2O is the dominant constituent, impurities can drastically alter the product yields (Spinks and Woods 1990). Therefore, the results given here only provide guidance, and laboratory measurements are required for icy satellite surface conditions. Below we discuss the products that can form in the presence of ices containing sulfur and carbon species or salt minerals.

20.5.2 Irradiation of SO_2 and Sulfur: Pure and in Ice

Frozen anhydrous SO_2 is a major surface species on Io (Chapter 14). Laboratory studies show that energetic heavy ion bombardment predominantly ejects the most volatile products, SO_2, SO, O_2 and, possibly, S_2 (Boring *et al.* 1984). The yields at low temperatures can also be scaled as in Figure 20.6 and are temperature dependent above ~80 K (Boring *et al.* 1986, Lanzerotti *et al.* 1982). Radiolysis of solid SO_2 also produces less volatile products SO_3 and S_x (Rothschild 1964, Moore 1984). These are formed and trapped in the irradiated samples altering their reflectance. Radiolytic darkening of deposited SO_2 may be occurring in Io's polar regions (Johnson 1997), as discussed below.

Sulfur is also found on Io's surface. Sputtering of cold cyclo-octal sulfur, S_8, by heavy ions produces S_x, with x = 1 to 8 and S_2 the dominant ejected species (Chrisey *et al.* 1988a). A sputter-resistant residue is formed that is like polymerized sulfur (Torrisi *et al.* 1988). The remaining sulfur is chemically changed, producing a brownish product thought to be sulfur fragments. These fragments are metastable and can recombine to form S_8 at temperatures of about 170 to 200 K (Chrisey *et al.* 1988a). Ultraviolet and X-ray irradiations produce similar coloration and visible absorbers (Nishijima *et al.* 1976, Casal and Scaino 1985, Steudal *et al.* 1986, Nelson *et al.* 1990). H_2S and sodium sulfides have also been suggested as possible constituents. These readily lose H_2 and Na leaving a sulfur residue and ejecting some S_2 (Chrisey *et al.* 1988b, Boring *et al.* 1985).

The icy satellite surfaces, particularly Europa, are thought to contain sulfur implanted from the magnetospheric plasma, and SO_2 has been proposed as a surface component of these bodies (Lane *et al.* 1981). Endogenic sources of sulfurous material such as sulfate salts, sulfides or acids are also possible. For the icy satellites, radiation-induced chemical reactions of sulfur, sulfides or SO_2 in water ice are much different than for the pure compounds. Sulfurous solutes can be attacked by OH and other radicals formed by H_2O radiolysis, and reactive sulfur compounds produced in radiolysis can react with H_2O. In addition, the loss of hydrogen under irradiation means that oxidized forms are heavily favored.

Radiolysis of sulfur grains in liquid or frozen water produces sulfuric acid through a chemical pathway thought to involve attack by OH radicals and formation of transient sulfinic acid (Donaldson and Johnston 1968, 1971, Della-Guardia and Johnston 1980, Carlson *et al.* 2002). The ef-

ficiency for H_2SO_4 production (Table 20.4) depends upon the grain size and is midway between uniform diffusion of radicals to grain surfaces and a constant source volume of reactants (Donaldson and Johnston 1968, Carlson *et al.* 2002).

Radiolysis of SO_2 in water ice was predicted to produce sulfuric acid through the rapid reaction of SO_3 with H_2O (Carlson *et al.* 1999b). Measurements by Moore *et al.* (2002) of proton-irradiated SO_2:H_2O mixtures at Europa-like temperatures have shown that sulfate is indeed produced. It is also produced by photolysis in a dilute mix of SO_2 in ice (Schriver-Mazzouli *et al.* 2003). Since sulfuric acid is hydrophilic, hydrated sulfuric acid will be the dominant end-product of sulfur and SO_2 radiolysis in excess ice. In turn, radiolysis of H_2SO_4 (back reactions) produces sulfur and SO_2, and a small amount of H_2S that is rapidly decomposed to sulfur (Wourtzel 1920, Boring *et al.* 1985). Sulfur is continuously cycled through these chemical forms, which we refer to as the radiolytic sulfur cycle (Carlson *et al.* 1999b, Carlson *et al.* 2002). Steady-state concentrations of H_2SO_4, SO_2, S_x, and H_2S will be formed in ice, with their relative abundance determined by production and destruction efficiencies. The concentrations predicted from these G-values are roughly consistent with the relative concentrations of SO_2, S_x, and sulfate on Europa (Carlson *et al.* 1999b, Carlson *et al.* 2002, Hendrix *et al.* 2002), as discussed below. Since the hydrate has a high sublimation energy and the hydrated water is more tightly bound than water molecules in ice (Novak 1974, Zeleznik 1991), it acts to lower sputtering and sublimation rates compared to ice. The radiolytically driven sulfur cycle could, of course, occur whether the sulfur came from endogenic or exogenic sources as discussed below.

20.5.3 Irradiation of CO_2 and Carbon Species in Ice

Implantation of carbon ions from the energetic plasma (Hamilton *et al.* 1981, Cohen *et al.* 2001) can be a source of carbon and CO_2 in the surfaces of the icy satellites (Strazzulla *et al.* 2003). Carbon in some form was likely present at formation and has since been delivered by meteoritic impacts. CO_2 has been seen trapped in the icy surfaces of Europa, Ganymede and Callisto (Carlson *et al.* 1996, McCord *et al.* 1997, McCord *et al.* 1998, Hibbits *et al.* 2000, Carlson 2001) and it has been seen as an atmospheric constituent at Callisto (Carlson 1999). Whereas irradiation of hydrocarbons produces H_2 and the growth of carbon chains, the presence of oxygen leads to more complex chemical pathways. In Table 20.5 are given the G-values for CO, CO_2 and a carbon suboxide. These are irradiated as condensed solids and in an ice matrix by energetic (0.8 MeV) protons and UV (10.2 eV) photons. As was the case for frozen SO_2, irradiation of frozen CO, CO_2 and carbonates can lead to ejection of CO_2, CO and O_2 and the production of more refractory species having carbon–carbon bonds. This consists of carbon sub-oxides (Chrisey *et al.* 1990, Gerakines and Moore 2001), such as C_3O_2 (Table 20.5), and a "dark" carbonized material (Strazzulla 1998). The latter does not form nearly as efficiently as when a hydrocarbon is irradiated (Lanzerotti *et al.* 1987). The sputtering yields for CO_2 and the relative amounts of CO produced depend strongly on the surface temperature (Brown *et al.* 1984, Schou *et al.* 1985, Brucato *et al.* 1997a). Both CO and O_2 produced at depth can diffuse to the surface and escape into the atmosphere.

Like SO_2, the radiation–chemical pathways for CO_2 in ice differ from that for pure CO_2 due to the availability of H. Therefore, carbonic acid is an important product, as is formaldehyde if the CO formed remains trapped (Moore *et al.* 1991, Pirronello *et al.* 1982, Brucato *et al.* 1997b). Similar to sulfur, carbon chains can form unless the CO_2 concentration is small (Hudson and Moore 1999). Delitsky and Lane (1997, 1998) have listed a plethora of organic molecules that might form by irradiating a mixture of carbon in ice. However, relative amounts are not given and laboratory reflectance measurements are needed to identify the suggested species. The ozone-like feature at Ganymede may include a band associated with a complex organic (Johnson 2001), an organic material has been suggested to be present on Europa (Dalton *et al.* 2003), and the dark material at Callisto has been proposed to be carbonized material (cf. Hibbitts *et al.* 2000, Carlson 2002b, Carlson *et al.* 2003a).

Ionizing radiation not only forms more complex molecules, it can efficiently decompose organics. At low doses, CO and CO_2 molecules are the principal decomposition products of a number of organics and carbonates (e.g., Calvert and Pitts 1996, Bernstein *et al.* 1995) and production of these species can be enhanced in the presence of oxygen. The photolysis of methanol in ice produces CO_2 (Ehrenfreund *et al.* 2001). Since CO_2 trapped in ice is seen on all three icy satellites, it could be in the form of an intrinsic clathrate (Moore *et al.* 1999). However, this structure is readily destroyed by ionizing radiation (Moore and Hudson 1994). The trapped CO_2 could also be due to implantation of carbon in ice (Strazzulla *et al.* 2003), but is more likely to be a decomposition product of an endogenic organic (Johnson 2001) or a carbonaceous material delivered by meteorites (Carlson 1999). Because ionizing radiation can both form and destroy complex hydrocarbons, a carbon cycle, like the sulfur cycle on Europa, must occur with CO_2, carbonates, and carbon sub-oxides as principal end-products (Johnson 2001). In regions having both carbon and sulfur, other molecules can be formed that include both species, such as OCS, CS_2, H_2CS, etc.

20.5.4 Irradiation of Salts and Acids

Models of the evolution of the Galilean satellites and their possible oceans suggest that salts may be important constituents (Fanale *et al.* 1974, Kargel 1991, Kargel *et al.* 2000). Alkali, alkaline-earth, and acidic sulfates, carbonates and chlorides have been proposed on theoretical and observational grounds. Such materials, if brought to the surface, are subject to radiolysis. At Io these minerals can be directly emplaced by volcanism. Because of the availability of excess sulfur, species such as Na_2S_x may also be present. On the surfaces of the icy satellites such materials may exist as hydrates or frozen brines. Radiolytic destruction can occur by decomposition of the anion or by removal of the cation, which may be neutralized or can react. Hydrates can also lose their water of hydration by sputter ejection or through radiolysis, producing O_2 and H_2.

Under irradiation, all of the suggested molecular compounds can decompose and change their reflectance (Nash and Fanale 1977, Wiens *et al.* 1997, Chrisey *et al.* 1988a).

Table 20.4. *G*-values for water and sulfur species.

Molecule	Radiation (reference)	T (kelvins)	Products	G $(100\ eV)^{-1}$	Parent Lifetime on Europa (Years)
H_2O	MeV H^+ (a)	16	H_2O_2	0.1	
H_2O	30 keV H^+, O^+, N^+, C^+, Ar^+(b)	16, 77	H_2O_2	0.10–0.26 0.06–0.34	
H_2O with ~10% CO_2	MeV H^+ (a)	77	H_2O_2	0.1	
H_2O with ~10% O_2	MeV H^+ (a)	77	H_2O_2	0.41	
H_2O	Ions, e, $h\nu$	7–120	O_2	4×10^{-5}–0.1	
S in H_2O ice	γ (c)	> 77	H_2SO_4	0.4	120
SO_2	MeV H^+ (d)	20, 88	SO_3	4.5	
	γ (e)	256	S	0.65	5
			O_2	0.01	
Sulfate	KeV e^- (f)	300	Sulfite	0.0034	
			Sulfide	0.000 64	3800
			S	0.000 08	
H_2S	α (g)	83	S	8	6

(a) Moore and Hudson 2000; (b) Gomis *et al.* 2004; (c) Carlson *et al.* 2002, the rate is particle size dependent, value for 50 μm radius particles; (d) Moore 1984; (e) Rothschild 1964; (f) Sasaki *et al.* 1978; (g) Wourtzel 1920.

Table 20.5. *G*-values for carbon oxides and carbonic acid.

	$G(CO)$		$G(CO_2)$		$G(C_3O_2)$		$G(H_2CO_3)$	
Initial Ice	H^+	UV	H^+	UV	H^+	UV	H^+	UV
CO^a			0.25(.04)	0.9(.2)	0.24(.04)	0.014(.001)		
$CO_2{}^a$	1.1(.1)	8.1(.3)			<0.001	<0.001		
$C_3O_2{}^a$	0.68(.04)	1.1(.1)	0.12(.02)	0.074(.004)	−4.3(.4)	−6.5(.4)		
H_2O+$C_3O_2{}^a$	0.063(.008)	0.045(.005)	0.019(.004)	0.13(.01)	−0.13(.01)	−0.47(.09)		
H_2O+$CO_2{}^b$ (1:1)	0.20(.07)	0.32(.15)	−0.55(.05)	−0.56 (.09)			0.028(.024)	0.030(.016)
H_2O+CO^c (5:1)	−0.7		0.16					

Negative values indicate destruction yields. UV photons are 10.2 eV (Lyman-α) and protons are 0.8 MeV. Parentheses give uncertainties. (a) Gerakines and Moore 2001; (b) Gerakines *et al.* 2000; (c) Hudson and Moore 1999.

This is clearly the case for energetic heavy ions that can fully dissociate any molecule penetrated, but is more problematic for lightly ionizing radiations, such as EUV photons and fast protons and electrons.

Sulfate is one of the most radiation resistant anions. Using electron paramagnetic resonance, a primary destruction path of SO_4^{2-} was found to be formation of the ion radical SO_4^- by either interaction with a hole or by direct ionization (Moorthy and Weiss 1964, Spitsyn *et al.* 1964). Subsequent recombination with an electron (Gromov and Morton 1966) produces sulfate in an excited state that can relax to the ground state or dissociate (Gromov and Karaseva 1967)

$$SO_4^- + e \rightarrow (SO_4^{2-})^* \rightarrow \begin{array}{l} SO_3^- + O^- \\ SO_3^- + e + O \\ SO_2^- + e + O_2 \\ SO_4^{2-} \end{array} \quad (20.1)$$

The branching ratio for dissociation is about 75% and occurs in the temperature range 100 to 140 K and higher (Gromov and Karaseva 1967, Barsova *et al.* 1969). The lifetime of an SO_3^- radical in water ice is a few days or less at europan temperatures (Ikeya *et al.* 1997). Efficiencies for SO_3^- production are reduced in hydrates, with G-values of 0.12 to 0.005 reported for anhydrous and hydrated $BeSO_4$, for example (Karaseva *et al.* 1973). The SO_2^- and SO_3^- ions can produce trapped SO_2 and SO_3 molecules (Karaseva *et al.* 1968, Gromov and Spitsyn 1969) that may slowly escape by diffusion (McCord *et al.* 2002).

Ion spectroscopy of sputtered sulfates show that O, SO^-, SO_3^-, SO_4^-, and the unresolved combinations O_2^{2-}+ S^- and S_2^- + SO_2^- are produced (Benninghoven *et al.* 1987). Sputtering of Na_2SO_4 produces sodium oxides, sulfides, and sulfoxides (Wiens *et al.* 1997). Photoelectron spectroscopy studies of Li_2SO_4 showed formation of sulfite (SO_3^{2-}), elemental sulfur (S), and sulfide (S^{2-}), with a total G-value for destruction of 0.0041 (Sasaki *et al.* 1978). Using the fluxes of Cooper *et al.* (2001) with $G = 0.0041$ gives a sulfate lifetime

at Europa of about 3800 years (Carlson *et al.* 2002). This G-value is consistent with the upper limit for one destruction channel, SO_2 production and escape, found by electron irradiation of hydrated and anhydrous $MgSO_4$ (McCord *et al.* 2001b, 2002).

Hydrated sulfates lose their water under irradiation, yielding H_2 and O_2. The efficiencies are less than those for water ice, generally being $G(-H_2O) < 0.01$. For $MgSO_4{*}7H_2O$, $G(-H_2O) = 0.003$ (Huang and Johnson 1965). Radiolysis of hydrated salts can alter the shape of the hydration bands, shifting band minima to shorter wavelengths and sharpening the high-frequency edge (Nash and Fanale 1977). These shifts and shape changes are similar to those found in thermal dehydration and must be considered when comparing jovian satellite and laboratory spectra (Dalton and Clark 1999, Dalton 2000). Few laboratory spectra exist for irradiated samples of candidate surface materials, so definitive identifications or limits cannot be made based on precise band positions.

The alkalis, which exist in these solids as singly-charged ions, are the most readily removed cation by the incident UV and particle radiation. That is, ionizing radiation produces excess electrons that attach to the alkalis causing desorption of a neutral (Yakshinskiy and Madey 1999). Although Mg, which is doubly ionized in these materials, is not as readily removed, it is present in the ejected ion spectra from hydrated sulfate salts (E. deSilveria 2000, private communication) and as an ejected excited neutral species from proton irradiation of epsomite ($MgSO_4{\bullet}7H_2O$) and bloedite $Na_2Mg(SO_4)_2\ {\bullet}4H_2O$ (Nash and Fanale 1977). The mineral cations in the salt may be replaced by H^+, which is readily available in an ice matrix. Therefore, highly hydrated salts might also yield hydrated sulfuric acid under the radiation conditions on Europa (Johnson 2001).

Sodium and potassium have been observed as atmospheric constituents at both Io and Europa, but magnesium atoms have not been detected, although they are suggested to be present in Europa's surface material. If Mg is present, decomposition could lead to the formation of MgO and/or $Mg(OH)_2$ in the surface (Johnson 2001). At Europa, upper limits have been placed on likely radiation products NaOH and $Mg(OH)_2$ of 5% and 3%, (by number), respectively (Shirley *et al.* 1999).

The observed, gas-phase sodium and potassium can be radiolytic products of the proposed sulfates, as seen clearly in laboratory experiments (Chrisey *et al.* 1988b, Wiens *et al.* 1997). However, recent observations of Io indicate that Cl atoms are present in comparable amounts (Kueppers and Schneider 2000). NaCl, recently observed at Io (Chapter 19), is also readily decomposed by ionizing radiation (e.g., Madey *et al.* 2002). Since it is also efficiently dissociated in Io's atmosphere, the sodium and chlorine react separately with the principal surface species, SO_2, or the latter's radiation products. Therefore, Cl_2SO_2 could be present on Io's surface (Schmitt and Rodriguez 2001) and likely is decomposed by ionizing radiation to Cl_2 and SO_2.

On the icy satellites, sputtered and redistributed alkalis that return to the surface can adsorb in icy regions. Although these adsorb as ionic species, they are readily removed radiolytically, a process referred to as electronically stimulated desorption (Yakshinskiy and Madey 2001, Madey *et al.* 2002). The loss of hydrogen under irradiation can result in the production of oxidized alkalis at depth in the material (Johnson 2001).

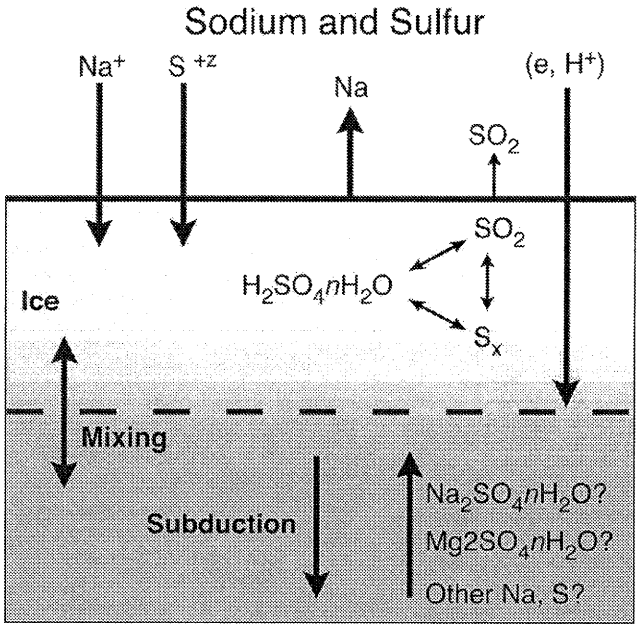

Figure 20.8. Schematic diagram of the processing of Europa's trailing hemisphere. The electrons and protons are the primary agents of radiolysis and the sulfur cycle is indicated. Sodium and sulfur may be implanted into the ice from the plasma or may come from subsurface sources as indicated. Na and O_2 have been seen as gas-phase ejecta, but volatiles H_2, H_2O, SO_2, and H_2S must also be present as well as CO_2 and CO from the leading hemisphere. Meteoriod bombardment mixes the irradiated layer and upwelling may bring new materials to the surface. nH_2O indicates a hydrate involving n water molecules.

20.5.5 Adsorption

Adsorption of a volatile in the presence of radiation can enhance erosion, a process often used to chemically etch refractory surfaces. That is, at temperatures well above sublimation temperatures, volatiles can adsorb on surfaces, particularly at radiation damage sites (Madey *et al.* 2002). Subsequent irradiation can lead to different chemical pathways than in the bulk material. Adsorption of water or oxygen on sulfur or carbon in the presence of radiation causes oxidation. The production and loss of SO and SO_2 or CO and CO_2 then results in the surface erosion. Similarly, implantation of reactive species, such as O and H, into sulfur or carbon can lead to the production and loss of volatiles (Brucato *et al.* 1997b).

20.6 SUMMARY OF SATELLITE IRRADIATION EFFECTS

In this section we review our understanding of the production of atmospheric species and the modification of the surfaces of the principal jovian satellites by radiolysis. The section on Europa is by far the largest since radiolysis occurs rapidly on this object, its surface appears to be young, and many of the issues discussed also relate to the other two

icy satellites. To guide the discussion, in Figure 20.8 we show schematically the processes involving sodium and sulfur in ice that occur in Europa's surface: the implantation of sodium and sulfur ions; the layer modified by penetrating energetic electrons and protons; the mixing downward of the irradiated layer by meteoroid bombardment; possible subsurface sources of sodium and sulfur; the ejection from the surface of the most volatile species, Na and SO_2; and the sulfur chemical cycle induced by the radiation. Such processes occur at some level on all of the satellites that orbit in Jupiter's radiation belt and, of course, must involve species other than sodium and sulfur. Grain charging and levitation must occur at some level on these objects, but is not discussed. The satellite geology, atmospheres and other surface modification processes are described in other chapters.

20.6.1 Metis, Amalthea and Thebe

The inner jovian satellites are discussed in Chapter 11. Here we note that Amalthea and Thebe are both very red showing a strong slope in the 0.25 to 0.45 μm spectral region. This, among other possibilities, could be suggestive of sulfur-bearing species (Gradie *et al.* 1980, Pascu *et al.* 1992). Like the Galilean satellites, their leading hemispheres are brighter than the trailing hemispheres by about a factor of 1.4 (Pascu *et al.* 1992). Although these observations show that the trailing side of Amalthea is slightly redder than the leading side, the opposite asymmetry was found for Thebe. Simonelli *et al.* (2000) showed 25–30% greater leading side brightness for these satellites as well as for Metis, one of two main-ring shepherds, the other being Adrastea. The main ring and the leading side of Adrastea were reddened by 15–20% at 1 and 2 μm (Meier *et al.* 1999).

Radiolytic modification of these surfaces has been suggested, but the common leading/trailing asymmetries for Metis, Amalthea, and Thebe argue for preferential meteoroid bombardment of the leading sides (Simonelli *et al.* 2000). However, the brightening mechanism is not understood. From *Pioneer 11* (Baker and Van Allen 1976) and *Galileo* (Fischer *et al.* 1996, Mihalov *et al.* 2000) data the fluxes for very high energy electrons and ions to these satellites are $\sim 10^{10}$–10^{11} keV $(\mathrm{cm}^{-2}\ \mathrm{s})^{-1}$ with likely higher inputs from 10 keV to 10 MeV particles, which typically carry most of the magnetospheric particle energy. Such fluxes could produce substantial chemical modification and perhaps darkening (depending on composition of irradiated material) in tens to hundreds of years at micron depths and thousands of years at millimeter depths. Even Adrastea, which lies inside the synchronous orbit, would be irradiated at saturation levels over the whole surface by the energetic particle flux. The common leading/trailing asymmetries for Metis, Amalthea, and Thebe argue for a strong effect from preferential meteoroid bombardment of the leading sides (Simonelli *et al.* 2000). Therefore, the asymmetries might arise from global darkening by the radiation, or another weathering agent, in competition with excavation of bright material on the leading side by meteoroid impact.

20.6.2 Io

Magnetospheric irradiation of Io's surface has a different character than that for either Europa (which is largely unshielded) or Ganymede (for which an internal dipole exists). For instance, energetic electron drift paths are diverted around the body at some energies (e.g., Thorne *et al.* 1999) rather than flowing directly on to the trailing hemisphere. Magnetic fields over the north and south polar regions, as measured during the I31 and I32 *Galileo* flybys, show little divergence from the background magnetospheric field (Chapters 21, 22), so surface irradiation may be greater there.

The discovery of the Io sodium cloud provided the first indication that atoms and molecules might be sputtered from its surface (Matson *et al.* 1974). Whereas sodium sulfides and sulfates were initially proposed as primary surface constituents (Fanale *et al.* 1974), the surface is now known to consist of various sulfur allotropes, SO_2, and some silicates (Chapter 14). Because the yields for sputtering of SO_2 are large (Lanzerotti *et al.* 1982), there was debate on whether Io's atmosphere was a thin sputter-produced atmosphere (Sieveka and Johnson 1985) or a thick sublimation and volcanic atmosphere (Chapter 19). Although sputtering of SO_2 may contribute in some regions, it is not the dominant atmosphere-forming process at Io.

Radiolysis of SO_2 is efficient, but volcanism rapidly resurfaces Io by deposition from plumes and by surface flows. Therefore, radiolytic products are not abundant in the optical layer except near the poles, where there are fewer volcanoes and a higher fraction of the incident particles reach the surface (Wong and Johnson 1996). Whereas early discussions of leading/trailing asymmetries focused on radiolysis (Burns and Matthews 1986), the rapid resurfacing suggests that at Io the observed differences are geological.

Sulfur trioxide and elemental sulfur are radiolytic products of SO_2. SO_3 is difficult to observe on Io in the near-IR because its band coincides with Io's strong SO_2 $\nu_1 + \nu_3$ band. However, a feature at 465 cm^{-1} in Io's thermal infrared spectrum suggests the presence of significant amounts of SO_3 (Khanna *et al.* 1995). Io's darker poles are likely due to sulfur chains produced by radiolysis of SO_2 molecules that migrate and condense at high latitudes (Johnson 1997, Wong and Johnson 1996). A broad 1-μm absorption band shows a polar enhancement (Carlson *et al.* 1997). This has been attributed to long-chained sulfur molecules (Carlson 2002b), based on spectral similarities to darkening agents produced in irradiated sulfates (Nash and Fanale 1977).

Although volcanic emission and sublimation (on the dayside) combined with gas-phase photolysis are major sources of atmospheric species, radiolytically produced volatiles, such as SO and O_2, might contribute on the nightside and at the poles (Wong and Smyth 2000). In addition, since Io's atmosphere is collisional everywhere, sputtering of the surface does not directly populate the Io torus. However, sputtering and decomposition likely contribute trace species (sodium, potassium and chlorine) to the atmosphere, which are then lost by the interaction with the magnetosphere. Therefore, the low sodium to potassium ratio seen in Io's extended atmosphere (e.g., Table 20.6) may be indicative of preferential loss of sodium by atmospheric escape. Sodium was initially thought to exist in the surface as Na_2SO_4 or

Table 20.6. Sodium to potassium ratio.*

Object		Na/K
Europa	Atmosphere	25
	Escape**	27
	Surface**	20
	Ocean***	14–19
Io	Atmosphere	10
Solar	Abundance	20
Lunar	Atmosphere	6
Mercury	Atmosphere	80–190

*From Brown (2001) unless otherwise indicated.
** Escape→ the ratio of Na to K escaping Europa's gravity (Leblanc *et al.* 2002).
***Model ocean value from Zolotov and Shock 2001.

NaS_x. But NaCl has been observed in Io's atmosphere (Lellouch *et al.* 2003) and Cl_2SO_2 was suggested as a possible surface species (Schmitt and Rodriguez 2001). These both readily decompose under ionizing radiation as discussed. The relative importance of volcanic and sputtering sources for trace atmospheric species is presently unknown.

20.6.3 Europa

Species detected in the optical surface of Europa are H_2O ice, a hydrated compound, H_2O_2, O_2, SO_2, and CO_2. Two kinds of visually dark material are found, one being dark in the UV (0.35 μm) and concentrated on the trailing side, while the second is brighter in the UV and preferentially distributed on the leading hemisphere (McEwen 1986). Elemental sulfur is a candidate for the first component (McEwen 1986, Johnson *et al.* 1988, Carlson *et al.* 1999b, Carlson *et al.* 2002) and the latter could be similar to the dark carbon-containing material discussed below for Ganymede and Callisto, but these identifications both need to be directly demonstrated. Oxygen, a sputter product from water ice (Johnson *et al.* 1982, 1983, 2003), is a principal atmospheric constituent (Hall *et al.* 1995, 1998, Kliore *et al.* 1997) and atomic Na and K are observed in the extended atmosphere (Brown and Hill 1996).

The depth of the optical layer in the IR (~1mm) is comparable to the mean stopping depth for energetic electrons (Cooper *et al.* 2001), so the spectroscopically-sensed surface is highly processed by the incident radiation. Given the short timescales for a significant dose (Figure 20.5), all molecules in this layer have suffered radiolytic action in <100 years. Temporal variations in absorption bands have been seen by the International Ultraviolet Explorer (IUE) (Domingue and Lane 1998a), and may indicate that surface concentrations can vary on short timescales due to magnetospheric variability. The supply and loss of sodium and sulfur, as indicated in Figure 20.8, and the irradiation processing and mixing loss of the surface layer are discussed below.

Hydrogen peroxide, a product of water radiolysis, can be dissociated by solar ultraviolet radiation. Therefore, its presence on a satellite surface implies a significant production rate (cf. Carlson *et al.* 1999a, Gomis *et al.* 2004). Europa's H_2O_2, observed in the infrared and ultraviolet, is concentrated on the leading, icy hemisphere and is enhanced in dark areas that also contain CO_2. The possible correlation of H_2O_2 with CO_2 (Carlson 2001) may be consistent with the laboratory measurements of Moore and Hudson (2000). They found that adding small amounts of O_2 and CO_2 to water ice greatly increased the H_2O_2 yield for MeV protons at 77 K. Since ~2/3 of the deposited energy is deposited below a photo-destruction layer ~200 μm in thickness (Figure 14 of Cooper *et al.* 2001), this oxidant must also exist at depth and could accumulate in buried reservoirs.

Molecular oxygen, initially observed at Ganymede via very weak absorption bands at 0.5773 and 0.6275 μm (Spencer *et al.* 1995), was also recently observed trapped in Europa's surface (Spencer and Calvin 2002). These bands are associated with two or more O_2 molecules trapped in a small volume where they absorb jointly. Their presence in Europa's spectra implies that a significant amount of O_2 must exist in the surface on both the leading and trailing hemispheres. Unlike at Ganymede, the band associated with O_3 is not seen, possibly due to the availability of S or because it is below the detection limit. Some of the surface-generated O_2 forms an atmosphere (Figure 20.8). The net escape rate is still highly uncertain: $\sim 2 \times 10^9$(Saur *et al.* 1998, Wong *et al.* 2004) to ~1–2 × 10^{10} cm^{-2} s^{-1} (Shematovich *et al.* 2004). For steady-state conditions, the latter implies a radiolytic production rate of O_2 due to the net energy deposited (Table 20.1) of $G(O_2) > \sim 0.01$ to 0.03. The larger atmospheric source rates appear to be supported by the recent observation of a neutral gas torus at Europa (Mauk *et al.* 2003) and may involve a considerable component of molecular hydrogen (Shematovich *et al.* 2004).

Iogenic sulfur, trapped in the jovian magnetosphere, is implanted into Europa's surface (Figure 20.8 and Table 20.3). This was thought to be the direct source of the UV absorption feature associated with SO_2 trapped in the ice (Lane *et al.* 1981). However, the UV absorption feature seen in the laboratory for sulfur ion implantation differed from those observations (Sack *et al.* 1992). Since H_2 is readily lost and mobile H is formed, oxygenated species will form (Johnson *et al.* 2003). However, the very stable sulfate hydrate may be a more likely end-product than SO_2 with the band seen in the laboratory as an intermediate species.

Much of Europa's surface is, in fact, covered with a hydrated compound, whose spectrum (Figure 20.9) looks nearly identical over the surface. This suggests that either one hydrated species is present or, if a mixture is present, it must be roughly the same everywhere. The hydrate distribution is centered on the trailing side and correlates with the UV dark material (Figure 20.2). Based on radiation chemistry arguments and spectral fits (e.g., Figure 20.9), this hydrated compound was reported by Carlson *et al.* (1999b) to be hydrated sulfuric acid. Although the fits are not perfect they may be improved by considering the spectral shifts and band profile changes caused by irradiation (Carlson *et al.* 1999b, Dalton 2000). The SO_2 and the spatially associated UV dark material, proposed to be sulfur chains (Johnson *et al.* 1988, Calvin *et al.* 1995), would be produced by radiolytic destruction of the acid (Carlson *et al.* 1999a, 2002, Figure 20.8).

An alternative interpretation of the observed hydrate spectrum suggests the presence of hydrated salt minerals or frozen brines on Europa's surface (McCord *et al.* 1998b, 1999, 2002). This interpretation is in part based on models for satellite evolution (Fanale *et al.* 1974, Squyers *et al.* 1983,

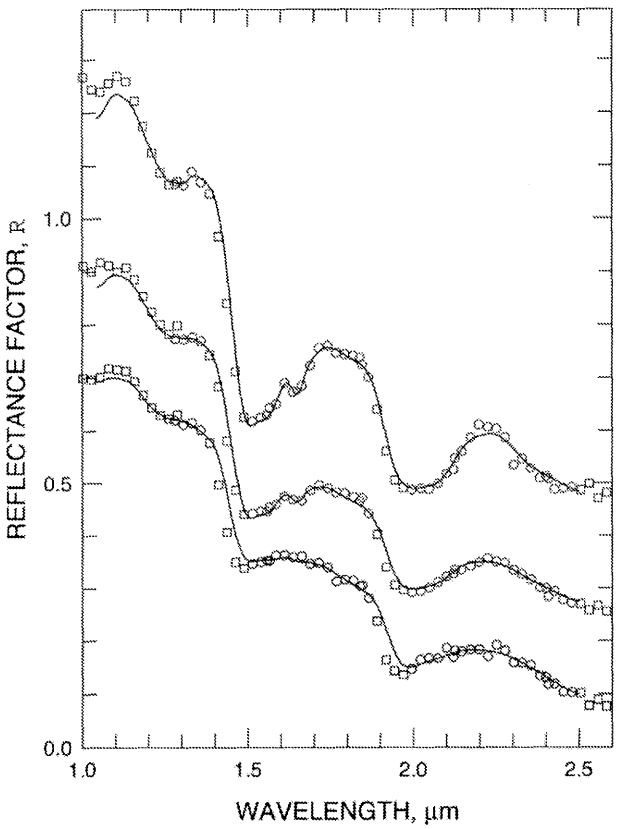

Figure 20.9. Europa NIMS spectra (circles and squares) and calculated spectral fits of hydrated sulfuric acid in water ice (Carlson *et al.* 2003b). The calculations assume intimate granular mixing and use measured complex indices of refraction for both materials. Data represented by circles are used in the fit. The bottom NIMS spectrum is fit with an acid volume fraction of 0.90, while the icier middle and upper spectra are found to have acid fractions of 0.54 and 0.30, respectively. Acid and ice grain radii are also derived and are typically 10 μm and 100 μm. Similar fits may be obtained with suitable mixtures of hydrated salts (McCord *et al.* 1999). The deviations from observations seen here are thought to be due to radiation-induced spectral shifts as observed in laboratory spectra of irradiated hydrates (Nash and Fanale 1977, Carlson *et al.* 1999b). Including a small admixture of hydrated salts, radiation damage to the ice (Dalton 2000) or a neutral scattering agent could, in principle, also improve the fits.

Kargel 1991). While no single mineral or single-component brine matches the observed spectra, specific mixtures of hydrated salts can provide a good spectral match (McCord *et al.* 1999). Variations in the mixture over the surface would have to be small in order to not significantly alter the spectra. This has been taken to indicate a uniformly mixed oceanic source (McCord *et al.* 1999). Spectra of hydrated salts exhibit structure that is not evident in NIMS spectra, but McCord *et al.* (2002), in attempting to simulate europan thermal and radiolytic effects in the laboratory, showed that this structure is diminished or absent in brines that were rapidly frozen (10 000 K min^{-1}) and subsequently heated to 230 K. They postulated that Europa's hydrate is hydrated $MgSO_4$ brine with a Na_2SO_4 contribution of <20%. Its presence on the surface would be due to emplacement of salts or brines by upwelling from Europa's ocean (Zolotov and Shock 2001), but the "salty" satellite models are still the subject of debate (McKinnon and Zolensky 2003). In addition, such salts will be chemically modified in Europa's radiation environment, as discussed above, with loss of the cation and the formation of sulfuric acid hydrate a likely result (Johnson 2001).

Sulfuric acid is found in the Venus clouds and as an aerosol in the Earth's atmosphere. Photochemical production occurs in both cases, although by different mechanisms and chemical pathways. Precipitation and thermal dissociation destroys the acidic particles and a steady state results from continuous production and destruction. Radiolysis acts similarly. Radiolytic cycling of sulfur (Figure 20.8) was proposed to be occurring in Europa's surface (Carlson *et al.* 1999b). Using the laboratory G-values in Table 20.4, the steady-state proportions of sulfur and SO_2 relative to H_2SO_4 by number are 10^{-2} and 10^{-3} respectively (for 50 μm sulfur particles). These are similar to the relative amounts derived from observations in three different spectral regions (Carlson *et al.* 2002). Spatial correlations are evident for the distributions of the UV dark material and the hydrate (Figure 20.2) and for SO_2 and hydrate distributions (Hendrix *et al.* 2002). H_2S, which would occur at the 2×10^{-4} level, has not been identified on Europa and may be below the detection threshold. Since the exposure times are long, the rapid processing can hide the identity of the "original" sulfur compounds. Therefore, one cannot establish the sulfur sources without further information.

Sulfurous materials that could, under irradiation, result in sulfuric acid hydrate and associated SO_2 and S_x can be exogenic or endogenic. Implantation of sulfur ions from the Io plasma torus (Lane *et al.* 1981), neutrals and particulates from Io (Domingue and Lane 1998a,b), and micrometeorite bombardment (Cooper *et al.* 2001) are exogenic sources. A subsurface ocean, either briny with sulfate salts (Kargel *et al.* 2000), acidic with H_2SO_4 (Kargel *et al.* 2001, Marion 2003) or containing sulfides, could also provide sulfur to the surface (Figure 20.8). It may be possible to discriminate between exogenic and endogenic sources using measurements of the spatial distribution of total sulfur, which is given by the distribution of the hydrate, since laboratory data indicate concentrations $[H_2SO_4 n H_2O] >> [S_x] > [SO_2] > [H_2S]$.

The global distribution of hydrate in Figure 20.2b shows a trailing-side enhancement that is similar to the plasma implantation distribution in Figure 20.4. These distributions are also similar to the well-known longitudinal distributions in reflectance in the visible and near-UV consistent with the presence of sulfur in the ice (Figure 20.2a, McEwen 1986, Johnson *et al.* 1988). As indicated in Table 20.3, more than enough sulfur is implanted to account for loss of sulfur to space. If undisturbed, Europa's trailing hemisphere could accumulate a 1-cm thick layer in about 10^7 years, ignoring plasma deflection. Therefore, the source must be reduced by deflection (e. g., Saur *et al.* 1998) or be buried by gardening (Carlson 2002a, Carlson *et al.* 2001, 2003b). Gardening can reduce the surface density of sulfur and increase the leading–trailing asymmetry as discussed. If Europa's ice shell is not tidally locked to Jupiter, then asynchronous rotation would *reduce* the asymmetry. The observed ratio of total sulfur at 180° W compared to 0° longitude is about 10. This is much less than the asymmetry ratio of 80 calculated assuming synchronous rotation and gardening (Carlson *et al.* 2003b).

Figure 20.10. Europa lineae and compositional variations. NIMS compositional map for approximately 182–188° W longitude, 4–10° N latitude overlayed on an SSI image. Hydrated material is shown as red, water ice is shown as blue. Note that the central bands of lineae are deficient in hydrated material compared to the margins. Heating (related to ridge emplacement) can darken the margins by sublimating ice and leaving a sulfurous lag deposit. At the time of going to press a colour version of this figure was available for download from http://www.cambridge.org/9780521035453.

Calculations using gardening rates from Cooper *et al.* (2001) and the spatial flux of sulfur ion implantation show that the observed distribution of total sulfur is consistent with an asynchronous rotation rate between 20 000 years and 2 Myr. Continuous churning of the surface by gardening gives a cumulative exposure time in the top 0.6 mm of more than 14 000 years or a dose greater than about 10^{25} eV cm^{-2}.

On a geologically inactive surface, implantation produces a spatial distribution of sulfur products that varies smoothly across the surface. However, this is not observed locally in high-resolution maps of the hydrate distribution, as seen in Figure 20.10. The distribution is variegated, particularly in the chaos regions, the regions modified by subsurface activity (Chapter 15). Features called triple bands are seen to exhibit diffuse margins containing the hydrate and the UV-dark material, presumably S_x. The central bands of the triple bands are remarkably deficient in both the hydrate and S_x, possibly indicating that material *upwelling* in the triple band centers is either *deficient* in sulfur or the sulfur is in some other form. If the upwelling materials were liquid brine, salts would rapidly drain downward reducing the salt concentration (Zolotov and Shock 2001), as in brine channel drainage found in terrestrial sea ice. The enhanced concentration of sulfur compounds along the margins of triple bands, in the chaos regions, and at pits, spots, and domes can be explained by thermal processing of a sulfurous surface. Diapirs rising from below can heat the surface, sublimating water molecules and increasing the concentration of less volatile sulfur compounds.

In this picture, the dark edges of the triple band are lag deposits of thermally concentrated, refractory residue S_x and sulfuric acid hydrate. Thus, implantation and heating (related to ridge emplacement) could in principle explain aspects of the observed distribution of sulfur compounds. Estimates of the atmospheric loss rate in Table 20.3 (Johnson *et al.* 2002) point to accumulation of implanted sulfur on Europa. However, additional internal sources of sulfur cannot be ruled out (Figure 20.8). Radiation processing of such material, particularly by the energetic electrons, also roughly correlates with the spatial distribution of the hydrate (Paranicas *et al.* 2001). Therefore, the triple band margins could be radiation and thermally processed minerals with the center consisting of a more dilute mineral–ice mixture.

Carbon dioxide is seen in the ice on the leading side of Europa and the distribution correlates with material dark at visual but not UV wavelengths on this hemisphere (Carlson 2001). This is suggestive of an irradiation-produced carbon cycle (Johnson 2001). Prompted by the possible radiolytic production of CO_2 on Callisto (see below), and noting that micrometeoroid in-fall is much greater on the leading side than on the trailing side, Europa's CO_2 could be formed by radiolysis of carbonaceous material brought in by micrometeoroids (Carlson 2001, 2002b, Carlson *et al.* 2003a).

Although they are trace species, sodium and potassium atoms have been observed as an extended, nearly toroidal, atmosphere at Europa (Chapter 19). These atoms are readily desorbed from salts and ices, as discussed, and are easily seen by their resonant fluorescence lines. Implantation from the jovian plasma torus has also been suggested as the source of Europa's alkalis (Brown and Hill 1996). However, modeling of the extended atmosphere gives a net atmospheric escape rate (Table 20.3) that exceeds the implantation rate and the other exogenic source rates given in Table 20.3 by an order of magnitude (Johnson 2000, Leblanc *et al.* 2002). In addition, in Table 20.6 are shown the sodium to potassium ratio in Europa's extended atmosphere and surface, as compared to ratios for other solar system objects. The ratio at Europa is more than a factor of two larger than it is in Io's extended atmosphere (Brown 2001, Johnson *et al.* 2002). These two pieces of evidence could suggest that the observed alkalis are from material intrinsic to Europa. Because incident flux is highly variable, as discussed, and the relative concentrations in the plasma have not been measured, this conclusion needs to be tested further. Zolotov and Shock (2001), assuming an ocean with sulfate salts, indicate that Na/K ratio of ~14–19 in Europa's putative subsurface ocean would be consistent with the observed surface ratio due to enhanced fractionation as material rises to the surface, but other satellite models are being considered (e.g., McKinnon and Zolensky 2003).

If indeed the alkalis are predominantly endogenic, then the observed sodium and sulfur might have different principal sources. Sodium atoms could predominantly come from a subsurface source with sulfur predominantly exogenic. Since chlorine has been observed at Io, frozen solutions of sodium chloride must be considered. Since this does not darken under irradiation, it could be present in the central band of the triple bands. If sodium is in fact endogenic, then the atmospheric loss rate could be used to estimate the supply rate to the surface. However, considerably more observations and improved models are needed.

Whether or not subsurface salts are the ultimate source

of alkalis, a large fraction (~70%) of the sputtered alkalis do not escape and return to the surface (Leblanc *et al.* 2002). Therefore, the redistributed alkalis are primarily desorbed from an ice matrix (Johnson 2000). This was shown by comparing ejecta velocity distributions obtained from models of the morphology of the sodium cloud with recent laboratory measurements of electronic sputtering of alkalis adsorbed on ice (Johnson *et al.* 2002, Yakshinskiy and Madey 2001). The ejection of sodium from ice was also shown to be more efficient (Yakshinskiy and Madey 2001) than it is from the suggested brines (Wiens *et al.* 1997). Using these measurements, the observed column of Na, and the atmospheric model, the globally averaged atomic concentration of Na in Europa's surface is ~0.008 (Leblanc *et al.* 2002).

Since sputtered and sublimated H_2O returns and sticks readily to the solid surface (Smith and Kay 1997), volatile radiolytic products, such as O_2 and H_2, can be important. The ejected H_2 is easily lost to space in spite of the low ejecta energies (Johnson 1998). Since H_2O sticks with unit efficiency, but O_2 does not, Europa's atmosphere is dominated by O_2 (Johnson *et al.* 1982). Other volatile products such as CO_2, SO_2 and H_2S should also be present in the atmosphere at concentrations higher than at the visible outermost layer of the solid surface, with O, CO and SO as primary dissociation products (Wong *et al.* 2004). H_2O, its dissociation products, and the ejected species discussed above likely produce a detectable Europa plasma torus (Schreier *et al.* 1993, Johnson *et al.* 1998, Shematovich *et al.* 2004).

Since Europa's surface is a porous regolith composed of ~50–100 μm grains, the effective source rates for Europa's atmosphere are also modified by sticking. Therefore, an H_2O molecule ejected in the regolith can stick on to a neighboring grain. Because of this, the effective H_2O yield from an icy satellite surface, averaged over angular incidence, is reduced from that for bombardment of a flat surface (Hapke 1986, Johnson 1989). Since O_2 does not stick to adjacent grains *it experiences no reduction*, enhancing its source rate relative to H_2O. Under ion bombardment O_2 can also *diffuse out* of a large grain (Benit and Brown 1990, Baragiola 2003). Therefore, although atmospheric models have typically used about 10–20% O_2 by mass, consistent with laboratory data at the average surface temperature (Johnson 1990), the effective O_2 source rates are likely comparable to those for H_2O. Complicating the modeling of the atmospheric source rate is the fact that H_2O sublimates and sputters from the hydrate much less efficiently than it does from ice. This will affect both the globally averaged (Table 20.2) and relative hemispherical erosion rates (Sieveka and Johnson 1982, Tiscareno and Geissler 2003). H_2 and O_2 production from the hydrate has not been measured and the returning O_2 can react with a radiation-damaged surface. This is of interest as HST observations show that excited oxygen is denser over Europa's icy regions (McGrath *et al.* 2000, 2002) in apparent contradiction to global models (Shematovich *et al.* 2004).

A striking feature on Europa is that the youngest areas of the surface on the trailing hemisphere exhibit the largest contrast, suggestive of an aging process. Surface aging could be due to mixing driven by micrometeorite bombardment or frost growth by redeposition. However, we note, as did Carlson *et al.* (2002), that radiolysis and thermal processing can mute or enhance the contrast. Therefore, the sulfur in the edges of the triple bands, which might be concentrated by heating, as discussed above, is eventually oxidized forming either SO_2 or hydrated sulfuric acid. This reduces the absorption in the visible. Therefore, including meteoroid mixing, the reduction in contrast in the youngest regions occurs over timescales that are geologically relevant as described earlier.

20.6.4 Ganymede

Ganymede possesses an internal magnetic field, so this satellite is at least partially shielded from energetic ion (<10 MeV) and electron impacts at equatorial to middle latitudes as discussed. This field may have varied in magnitude and dipole polarity over millions of years as in the case of Earth (Cooper *et al.* 2001). Particle precipitation along the open field lines at the poles is suggested by auroral observations of oxygen in the visible and UV (Chapter 19). In addition, the albedo changes close to those latitudes where the transition from open to closed magnetic field lines occurs might be due to spatial variations in particle precipitation (Johnson 1997, Pappalardo *et al.* 1998, Hansen and McCord 2004).

Despite the magnetic shielding, Ganymede's surface has spectral features resembling those on Callisto and perhaps on Europa. Therefore, sulfur ion implantation might account for the hydrated material on the trailing side in the form of hydrated sulfuric acid. The analysis by McCord *et al.* (2001a,b, 2002) inferred the existence of a frozen brine, possibly emanating from a subsurface ocean on Ganymede. Although chemical exchange of the putative subsurface ocean with the surface is much less likely at Ganymede than at Europa, liquid water might have flowed on to the surface in the past (Chapter 16). The identity of the observed hydrate is, therefore, not established but could also arise from plasma bombardment, as suggested by the trailing-side pattern.

Trapped CO_2 is present in Ganymede's surface material and has a patchy distribution, generally correlated with dark material as at Europa. This material has a different spectral slope in the visible than that of the principal absorber at Europa. Adopting the radiolytic CO_2 production mechanisms proposed for Callisto (see below), we suggest that Ganymede's carbon dioxide is likely produced by radiolysis of an icy carbonaceous surface. Implantation is not a likely source unless there is a relatively high abundance of carbon ions at energies below 10 keV, where Ganymede's magnetic shielding is less effective (Cooper *et al.* 2001). The carbon could be endogenic or exogenic and the energetic particles that produce this radiolysis may be contained in Ganymede's own magnetosphere. The absorption bands at 3.88 μm and 4.57 μm are discussed in the Callisto section.

The identification of gas-phase oxygen in Ganymede's polar atmospheres (Hall *et al.* 1998) indicates that radiolysis is occurring. This is also indicated by absorption bands associated with condensed O_2, primarily at mid-latitudes on Ganymede (Calvin *et al.* 1996, Spencer *et al.* 1995). A broad band at ~260 nm has been suggested to be O_3 trapped in ice (Nelson *et al.* 1987, Noll *et al.* 1996). O_3 is a radiolytic product of condensed O_2 but not a direct product of water ice, as discussed. The observed O_3-like absorption band, obtained by taking the ratio of the reflectance from the trailing and leading hemispheres, clearly contains one or more additional absorbers. OH was initially proposed (Noll *et al.* 1996), but

using a better description of the trapped O_3 band a hydrocarbon was recently suggested to be present (Johnson 2001).

The UV spectrometer on *Galileo* showed that a broad absorption feature in the spectral region where O_3 absorbs is strongest at latitudes that are higher than the solid-O_2 feature. This was attributed to enhanced production of O_2 at mid-latitude temperatures and to differences in path lengths at low and high latitudes for visible and UV photons (Johnson and Jesser 1997, Johnson and Quickenden 1997). Alternatively, it has been suggested that there are very cold regions (~30 K) on Ganymede's surface in which solid oxygen is stable (Vidal *et al.* 1997, Baragiola and Bahr 1998). The O_3-like feature appears to exhibit a morning side enhancement (Hendrix *et al.* 1999a), whereas the solid-O_2 feature appears to exhibit an afternoon enhancement (Spencer and Klessman 2001). These effects are not yet understood, although the solar UV would effectively dissociate radiolytically formed O_3, and diffusion of O_2 from depth is enhanced by warming of the surface. Finally, the observation of a strong UV slope below 230 nm (Burns and Matthews 1986) may also be consistent with the occurrence of radiolytic products such as H_2O_2 and O_2H (Taub and Eiben 1968, Carlson *et al.* 1999a, Hendrix *et al.* 1999b).

A visible line from atomic oxygen is seen in Ganymede's atmosphere at equatorial latitudes, primarily on the trailing hemisphere (Brown and Bouchez 1999) and atomic H has been seen globally (Barth *et al.* 1997). Depending on the temperature and the ice coverage, Ganymede's atmosphere may be dominated by H_2O on the dayside at low latitudes but is certainly dominated by O_2 elsewhere (Wong *et al.* 2004). However, such models cannot predict the H (9×10^{12} cm^{-2}) to O_2 (10^{14}–10^{15} cm^{-2}) ratio without a direct surface (radiolytic) source of hydrogen. Using the amount of O_2 associated with the observed hydrogen requires larger O_2 source rates than initially suggested (Barth *et al.* 1997) as also proposed for Europa (Shematovich *et al.* 2004). This is likely due to the fact that the O_2/H_2O ratio for the surface source was underestimated, as discussed above. A good model of the spatial distribution of the flux of ions and electrons to Ganymede's surface is needed to better describe the radiolytic production of atmospheric gases.

20.6.5 Callisto

Callisto possesses an ancient, dark surface, with ice exposed by impact craters and on some crater walls. In addition, the surface exhibits ice pinnacles indicative of extensive weathering (Chapter 17). Although the *Galileo* magnetometer data suggest that there also may be a subsurface ocean within Callisto (Khurana *et al.* 1998), there is no evidence that the putative ocean material has directly emerged on the surface. Carbon dioxide has been identified in both the surface (Carlson *et al.* 1996, McCord *et al.* 1997, 1998a, Hibbitts *et al.* 2000) and atmosphere (Carlson 1999) using *Galileo* NIMS data. Other bands are also present in Callisto's IR spectra but their identifications are not as well established. The global spatial distribution of the CO_2 and its presence in fresh craters has led to suggestions of exogenic and endogenic sources (Hibbitts *et al.* 1999).

The escape rate of Callisto's CO_2 atmosphere is estimated to be $\sim 6 \times 10^6$ cm^{-2} s^{-1}. The source of atmospheric CO_2 could be outgassing, cometary delivery, impact production, implantation, or radiolysis and photolysis. Surficial CO_2 is seen to be concentrated on the trailing side (Hibbitts *et al.* 2000). This leads to a slightly larger atmosphere on the trailing hemisphere (Wong *et al.* 2004) consistent with a slightly more robust ionosphere (Kliore *et al.* 2002). The hemispherical distribution is also similar to Europa's and Ganymede's hydrate. Therefore, radiation alteration is likely to be important on Callisto also. Although the radiolysis dose rates are much lower than at Europa, the surface is older and photolysis may be more important, hemispherical differences should again be enhanced by meteoroid mixing. Since the regolith growth rate seen in Figure 20.5 is much faster than the radiolysis rate, production of observable new species in the optical layer is severely limited on the leading hemisphere.

CO_2 molecules can be produced by the photolysis and radiolysis of many organic molecules that may be intrinsic or delivered by comets and meteoroids to the surface (Bernstein *et al.* 1995, Johnson 2001, Ehrenfreund *et al.* 2001). Cooper *et al.* (2001) inferred that a radiolytic efficiency of $G(CO_2) > 0.003$ (e.g., Figure 20.7) is needed to supply the atmosphere. Under irradiation, trace amounts of carbon-containing material on a silica gel produced CO_2 with a $G = 15$ (Krylova and Dolin 1967), and organics decompose giving CO_2 with much lower but still robust G values (Spinks and Woods 1990). It has been suggested that the carbonaceous surface layer arises from meteoroid in-fall, although organics intrinsic to Callisto and implantation cannot be ruled out.

Alternatively, the weathering that has evidently occurred on Callisto could be due to outgassing of CO_2 from primordial materials (Moore *et al.* 1999). Assuming such a CO_2 source, the plasma bombardment has been suggested to cause the CO_2 to trap more effectively on the trailing hemisphere (Hibbitts *et al.* 2000). Indeed, radiation causes additional trapping sites but it also makes trapped volatiles mobile (Benit and Brown 1990). Therefore, formation of the carbon dioxide by radiolysis and meteoroid-induced mixing may more likely account for the differences between hemispheres.

If CO_2 is produced by radiolysis then both CO and O_2 will also be products. Trapped O_2 has recently been detected in Callisto's surface (Spencer and Calvin 2002). CO may be produced directly or by gas-phase photolysis of ejected CO_2 leading to a global atmosphere dominated by CO (Wong *et al.* 2004). However, CO has not yet been identified in the surface or atmosphere. Water sublimation can lead to comparable amounts of H_2O in the atmosphere, but the amount of surface water existing as ice and not tied up as a hydrate is uncertain.

In the presence of water, irradiation of absorbed or trapped CO_2 can produce hydrocarbons, as discussed above, and a carbon cycle, like the sulfur cycle at Europa, can occur (Johnson 2001). Evidence for a hydrocarbon band exists in Callisto's spectrum (McCord *et al.* 1997). Irradiation of CO_2 in water ice yields carbonic acid, H_2CO_3 (Moore and Khanna 1991, Brucato *et al.* 1997b, Gerakines *et al.* 2000). This molecule produces an absorption band at 3.88 μm. Such a feature is found in NIMS spectra of both Callisto and Ganymede, as seen in Figure 20.11 (Hage *et al.* 1998, Carlson 2002a). The apparent match in band position is consistent with radiolysis occurring on Callisto (Carlson *et al.* 2003a). An alternative identification for this band is an

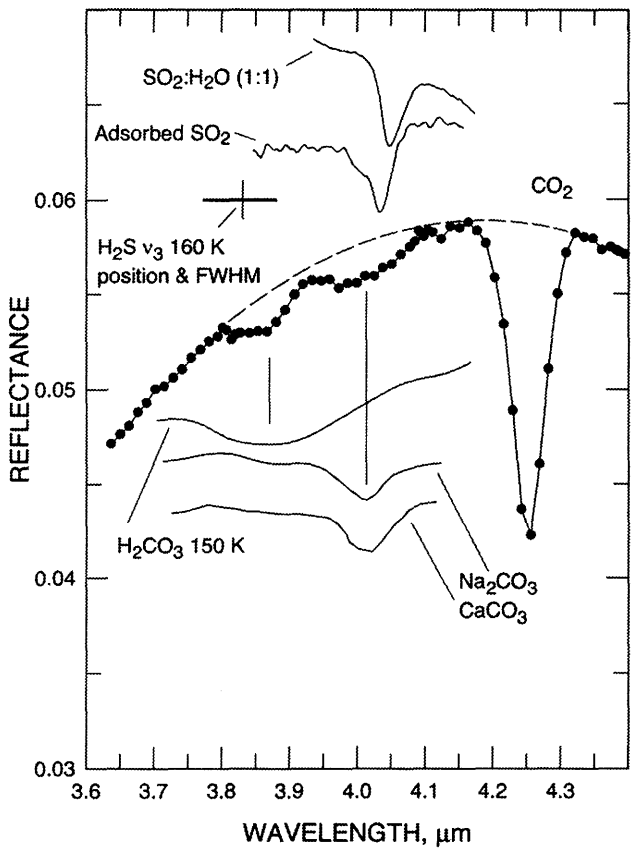

Figure 20.11. Callisto spectrum and candidate surface materials. A portion of Callisto's geometric albedo spectrum (filled circles, from Appendix A) is shown with a fitted quadratic continuum (dashed line). Representative spectrum (from 309 to 332° W, −15 to 20° N, phase angle ~62.8°) normalized to geometric albedo. Relative comparison spectra were derived from reflectance or absorbance data. Absorption by surficial CO_2 is evident in the NIMS spectrum along with two other bands whose source is not established. The band at ~3.87μm is associated with either a hydrosulfide, −HS (McCord *et al.* 1997, 1998b), or with radiolytic carbonic acid, H_2CO_3 (Hage *et al.*, 1998). Positions for H_2S (Schmitt *et al.* 2001) and H_2CO_3 (Gerakines *et al.*, 2000) are indicated. The absorption band at ~4.02 μm may be from SO_2 (McCord *et al.* 1997, 1998b) or carbonates (Carlson 2003a). Positions and shapes are shown for SO_2 in water ice (Moore *et al.* 2002), and for SO_2 adsorbed on Cabosil (Nash and Betts 1995). Carbonate absorptions are from Nyquist *et al.* (1997).

S–H stretch in a hydrosulfide (McCord *et al.* 1997, 1998a). This identification was suggested by the fact that sulfur is also implanted at Callisto and by the reported observation of SO_2 in the UV on the leading hemisphere of Callisto. However, OH and organics also absorb in this region of the UV. Therefore, although sulfur could be present, Callisto's surface is likely dominated by a carbon cycle with the principal dark refractory species being carbon and carbon sub-oxides seen as radiation products in laboratory experiments (Gerakines and Moore 2001). A band at 4.57 μm that may be due to C_3O_2 has been noted in NIMS spectra of Callisto (Carlson 2002a, 2002b, Carlson *et al.* 2003a). Rough *G*-values are given in Table 20.5.

20.7 SUMMARY AND IMPLICATIONS

It is now clear that a number of spectral characteristics of the surfaces of the Galilean satellites are likely determined by radiolysis caused by the impacting energetic ions and electrons trapped in the jovian magnetosphere. Radiolytic and photolytic processing of satellite materials alters the volatility of the surfaces and affects the composition of their atmospheres. At this time, the leading/trailing asymmetries seen on the icy Galilean satellites in the IR, in the visible and in the near-UV appear to be due to competition between the radiolytic formation of sulfur or carbon products in ice and micrometeoroid mixing of the surface material. The latter dominates on the leading hemispheres and the former on the trailing hemispheres. This contrast is probably modified by asynchronous rotation of the crust at Europa and the control of the plasma flow by the magnetic field at Ganymede.

The materials subjected to radiolysis and photolysis may be intrinsic to the satellite or they may be materials delivered by meteoroids, by particulates from neighboring satellites or by ion implantation of reactive species. Therefore, the reflecting layer is, at least in part, a patina produced by exogenic agents. Even materials of astrobiological interest may have been delivered by comet impacts (Pierazzo and Chyba 2002) and modified by radiolysis and photolysis (Dalton *et al.* 2003). With the exception of Io, where the surface is predominantly formed from endogenic material, the radiation timescales on the icy satellites can be fast compared with geologic processes. Therefore, separating exogenic and endogenic materials is a difficult but important task if one wishes to use remote sensing to understand the composition and evolution of the icy Galilean satellites. To this end, a significant modeling effort will be needed to unravel the radiolytic processing of the satellite surfaces. This will require planning and coordinating new remote sensing and laboratory observations. Comparisons of *Voyager* and *Galileo* plasma and reflectance data, and the many years of IUE reflectance data, all suggest that short-term variability is occurring in some form on the icy satellite surfaces and in their atmospheres. Therefore, with appropriate modeling and laboratory measurements, key observations can be suggested which might help separate endogenic and exogenic materials.

New laboratory measurements are needed on the irradiation of ices with contaminants and of those hydrated materials that have been proposed to be present. Based on the above discussion, ice containing both elemental sulfur and carbon or SO_2 and CO_2 should be studied. Also laboratory and field experiments on the formation and persistence of radiolytic products in *bulk* ice, and not just on thin films as in most laboratory experiments on sputtering and radiolysis, may be needed. Bulk irradiation by highly penetrating electrons and gamma rays is a standard commercial procedure for sterilization of materials and, therefore, may be useful for jovian satellite studies.

Increased effort is also needed at observing species in the tenuous satellite atmospheres and local plasma. These atmospheres will likely contain characteristic species other than the few already detected in the surface and the atmosphere, and any endogenic species might be more clearly identified in the gas phase. Large organic and perhaps even biological molecules that might reach the surface, where they would

typically be decomposed by the radiation, can be sputtered into the atmosphere as whole molecules by the energetic heavy ions bombarding Europa (Johnson *et al.* 1998). Since a number of the processes discussed cause isotopic fractionation, signatures in the plasma or atmosphere of isotopic abundances would be useful.

Although our emphasis has been on the chemical alteration of the optical layer, the presence of radiolytic products at depth is also of interest. For example, peroxide molecules are dissociated by the solar UV to depths of about 200 μm, but energetic electrons might produce peroxide at much greater depths as indicated in Figure 20.7. The depth range of peroxide is enhanced by meteoritic burial. Therefore, reservoirs of less volatile radiolytic products, such as OH radicals, H_2O_2 and hydrated minerals, will accumulate at greater than meter depths over the surface age of each satellite. Volatile products (O_2, CO_2) might also accumulate if they can trap in voids, so that the column densities observed by remote sensing are lower limits to total column abundances. Therefore, work is needed on both the retention and transport of volatile products within *bulk* ice samples subjected to time-variable temperature gradients and impact gardening. Indeed, field experiments on the trapping of volatiles in ice, on transport of species through brine channels and on retention of salts during freezing may be relevant.

Any landed mission to the icy Galilean satellites should attempt to obtain depth profiles of radiolytic products. Such vertical density gradients can provide information on the time history of the surface, interior heating of radiation products, and the potential transport of radiolytic resources to astrobiological niches. If an effective subduction process is operative for downward mixing from meter to kilometer depths, Europa's ocean could be fully oxygenated at terrestrial ocean levels using the upper limits in Cooper *et al.* (2001), while even lower oxygenation might still support microbial life (Chyba 2000). This would be analogous to the surface–interior exchange of nutrients and wastes that has been essential for evolution of life on Earth (e.g., Lovelock 1988). *Galileo* images of the surface suggest that the geologic component of such an exchange might be operative on Europa (Chapter 15) and possibly in young areas of Ganymede (Chapter 16). No such regions on Callisto have been identified (Chapter 17), but there could possibly be upward diffusion of CO_2 from subsurface sources.

Although coupling between the subsurface and surface materials might be active on the icy satellites, as is the case at Io, the available spectral evidence does not by itself confirm that such processes are operating. To date, the most compelling evidence for existence of subsurface oceans is from the *Galileo* magnetometer observations (Chapter 21). Geological evidence and crater counts argue for activity within the last tens of millions of years on Europa and billions of years ago on Ganymede (Chapter 18). Therefore, the most important objective for a future orbiter mission is to confirm the presence of a modern ocean as argued in the recent decadal reports on Europa exploration (Cooper *et al.* 2002, Belton *et al.* 2002).

With the possible exception of the alkalis at Europa, radiolysis or materials delivered by either implantation or meteoroids may be able to explain most features of the icy Galilean satellites. Therefore, there is at present no unambiguous compositional evidence that surface materials other than ice are intrinsic to these bodies, although we presume that such materials, if they are present, can be revealed. These discussions are, of course, preliminary and await additional mining of the large *Galileo* data set and better modeling of the radiolytic processing of the surface (e.g., Johnson *et al.* 2003). This modeling will hopefully motivate new observations that can test whether or not remote sensing can be used to understand the satellites' present state and evolution. It might also be able to impact on the possibility of materials from the putative subsurface ocean being emplaced on the icy satellite surfaces and the possible presence of biologically relevant materials. Since the radiolytic processing discussed is likely occurring on other outer solar system bodies, understanding its role in the jovian system can be critical to interpreting the reflectance spectra from more distant objects and for understanding the expected *Cassini* data.

20.8 SOME IMPORTANT ISSUES AND QUESTIONS

To assess the long-term effects of radiolysis on satellite surface materials and surface features, experimental measurements of molecular production and destruction rates at relevant compositions and temperatures are needed. In addition, we need assessment of radiation-induced wavelength shifts of spectral bands for remote sensing identifications and diagnostics. Specific issues are:

- What are the origins of the carbon, sulfur and alkalis already identified and what other important elements are present?
- Is there identifiable material transport to the icy satellite surfaces by rising ice diapirs or direct outflows from their putative subsurface oceans?
- In the presence of radiolysis and photolysis can endogenic and exogenic species be separately identified?
- What are the relative roles of sublimation, sputtering and outgassing for populating the atmosphere and torus, and for molecular transport across the surface?
- To what extent are species in the icy satellite atmospheres, in the neutral gas tori, and in the plasma diagnostic of the surface composition and resurfacing rates? Can trace surface species be identified in these regions?
- What can be learned from laboratory and field ice experiments that would help us understand the spatial and chemical distributions of radiolytic products on irradiated surfaces of the icy jovian and saturnian moons?
- Can radiolysis produce disequilibrium molecules in sufficient quantity to fuel biotic activity, and if bio-materials are emplaced on an icy satellite surface, what signatures might remain after radiolysis and photolysis?

Not only are laboratory studies needed to provide data on physico-chemical processes that effect the satellites, but the development of more detailed ion energy spectra by species and charge state are needed from eV energies upwards, particularly at low energies. These are needed in order to address interactions with the local fields and atmospheres and to better determine the energy and implantation flux to the satellite surfaces.

Acknowledgements. The authors would especially like to thank J. B. Dalton for two extensive reviews of this chapter and also acknowledge very helpful comments from T. B. McCord, T. M. Orlando, T. I. Quickenden, G. Strazzulla and F. Bagenal. JFC: NASA Office of Space Science through Raytheon from the Jovian System Data Analysis Program, Planetary Atmospheres Program, Space Science Data Operations Office at GSFC. MHM: NASA's Laboratory for Planetary Atmospheres and SARA Programs. REJ: NASA's Planetary Geology and Geophysics Program and the NSF Astronomy Program. RWC: NASA's Planetary Geology and Geophysics Program. CP, MCW, MHM, RWC: acknowledge institutional support from NASA.

REFERENCES

Bagenal, F., Empirical model of the Io plasma torus: *Voyager* measurements, *J. Geophys. Res.* **99**, 11 043–11 062, 1994.

Bahr, D. A., M. Famá, R. A. Vidal, and R. A. Baragiola, Radiolysis of water ice in the outer solar system: Sputtering and trapping of radiation products, *J. Geophys. Res.* **106**, 33 285–33 290, 2001.

Baker, D. N. and J. A. van Allen, Energetic electrons in the jovian magnetosphere, *J. Geophys. Res.* **81**, 617–632, 1976.

Bar-Nun, A., G. Herman, D. Laufer, and M. L. Rappaport, Trapping and release of gases by water ice and implications for icy bodies, *Icarus* **63**, 317–332, 1985.

Baragiola, R., Microporous amorphous water ice films and astronomical implications, in *Water in Confining Geometries*, J. P. Delvin and B. Buch (eds), Elsevier, 359–395, 2003.

Baragiola, R. A. and D. A. Bahr, Laboratory studies of the optical properties and stability of oxygen on Ganymede, *J. Geophys. Res.* **103**, 25 865–25 872, 1998.

Baragiola, R. A., C. L. Atteberry, D. A. Bahr, and M. Peters, Reply to comment by R. E. Johnson on "Laboratory studies of the optical properties and stability of oxygen on Ganymede" by R. A. Baragiola and D. A. Bahr, *J. Geophys. Res.* **104**, 14 183–14 187, 1999.

Baragiola, R. A., R. A. Vidal, W. Svendson, J. Schou, D. A. Bahr, and C. L. Atteberry, Sputtering of water ice, *Nucl. Instrum. Methods B* **209**, 294–303, 2003.

Barbosa, D. D., Stochastic acceleration of energetic ions in Jupiter's magnetosphere, *J. Geophys. Res.* **99**, 13 509–13 520, 1994.

Barsova, L. I., B. G. Ershov, G. Y. Popova, and V. I. Spitsyn, Investigation of the mechanism of formation of paramagnetic centers in g-irradiated alkaline earth sulfates, *Doklady Physical Chemistry* (translation) **184**, 108–111, 1969.

Barth, C. A., C. W. Hord, A. I. F. Stewart, W. R. Pryor, K. E. Simmons, W. E. McClintock, J. M. Ajello, K. L. Naviaux, and J. J. Aiello, *Galileo* ultraviolet spectrometer observations of atomic hydrogen in the atmosphere at Ganymede, *Geophys. Res. Lett.* **24**, 2147, 1997.

Belton, M., *New Frontiers in the Solar System: An Integrated Exploration Strategy*, National Research Council, 2002.

Benit, J. and W. L. Brown, Electronic sputtering of oxygen and water molecules from thin films of water ice bombarded by MeV Ne^+ ions, *Nucl. Instrum. Methods Phys. Rev. B* **46**, 448–451, 1990.

Benit, J., J. P. Bibring, S. della-Negra, Y. LeBeyec, M. Mendenhall, F. Rocard, and K. Standing, Erosion of ices by ion irradiation, *Nucl. Instrum. Methods Phys. Rev. B* **19/20**, 838–842, 1987.

Benninghoven, A., F. Rudenaur, and H. Werner, *Secondary Ion Mass Spectrometry: Basic Concepts, Instrumental Aspects, Applications and Trends*, Wiley, 1987.

Bernstein, M. P., S. A. Sandford, L. J. Allamandola, S. Chang, and M. A. Scharberg, Organic compounds produced by photolysis of realistic interstellar and cometary ice analogs containing methanol, *ApJ* **454**, 327–344, 1995.

Boring, J. W., J. W. Garrett, T. A. Cummings, R. E. Johnson, and W. L. Brown, Sputtering of solid SO_2, *Nucl. Instrum. Methods Phys. Res. B* **1**, 321–326, 1984.

Boring, J. W., Z. Nansheng, D. B. Chrisey, D. J. O'Shaughnessy, J. A. Phipps, and R. E. Johnson, The production and sputtering of S_2 by keV ion bombardment, in *Asteroids, Comets, Meteors II*, p. 229, 1985.

Brown, M. E., Potassium in Europa's atmosphere, *Icarus* **151**, 190–195, 2001.

Brown, M. E. and R. E. Hill, Discovery of an extended sodium atmosphere around Europa, *Nature* **380**, 229–231, 1996.

Brown, M. E. and A. H. Bouchez, Observations of Gonymede's visible aurorae, *BAAS*, **31**, 70.08, 1999.

Brown, R. A. and F. H. Chaffee, High-resolution spectra of sodium emission from Io, *ApJ* **187**, L125–L126, 1974.

Brown, W. L., L. J. Lanzerotti, J. M. Poate, and W. M. Augustyniak, "Sputtering" of ice by MeV light ions, *Phys. Rev. Lett.* **40**, 1027–1030, 1978.

Brown, W. L., W. M. Augustyniak, E. Simmons, K. J. Marcantonio, L. J. Lanzerotti, R. E. Johnson, C. T. Reimann, G. Foti, and V. Pirronello, Erosion and molecular formation in condensed gas films by electronic energy loss of fast ions, *Nucl. Inst. Meth. Phys. Res. A* **198**, 1–8, 1982.

Brown, W. L., W. M. Augustyniak, K. J. Marcantonio, E. H. Simmons, J. W. Boring, R. E. Johnson, and C. T. Reimann, Electronic sputtering of low temperature molecular solids, *Nucl. Inst. Meth. Phys. Res. B* **1**, 307–314, 1984.

Brucato, J. R., A. C. Castorina, M. E. Palumbo, M. A. Satorre, and G. Strazzulla, Ion irradiation and extended CO emission in cometary comae, *Planet. Space Sci.* **45**, 835–840, 1997a.

Brucato, J. R., M. E. Palumbo, and G. Strazzulla, Carbonic acid by ion implantation in water/carbon dioxide ice mixtures, *Icarus* **125**, 135–144, 1997b.

Burns, J. A. and M. S. Matthews, eds, University of Arizona Press, 1986.

Calvert, J. G. and J. Pitts, *Photochemistry*, John Wiley, 1996.

Calvin, W. M., R. N. Clark, R. H. Brown, and J. R. Spencer, Spectra of the icy Galilean satellites from 0.2 to 5 micron: A compilation, new observations, and a recent summary, *J. Geophys. Res.* **100**, 19 041–19 048, 1995.

Calvin, W. M., R. E. Johnson, and J. R. Spencer, O_2 on Ganymede: Spectral characteristics and plasma formation mechanisms, *Geophys. Res. Lett.* **23**, 673–676, 1996.

Carlson, R., A tenuous carbon dioxide atmosphere on Jupiter's moon Callisto, *Science* **283**, 820–821, 1999.

Carlson, R., Spatial distribution of carbon dioxide, hydrogen peroxide, and sulfuric acid on Europa, *BAAS* **33**, 47.02, 2001.

Carlson, R., Radiolysis and chemical weathering on the Galilean satellites, *Eos* pp. P52C–06, 2002a.

Carlson, R., The diverse surface compositions of the Galilean satellites, in *Solar System Remote Sensing*, p. 9, 2002b.

Carlson, R., W. Smythe, K. Baines, E. Barbinis, K. Becker, R. Burns, S. Calcutt, W. Calvin, R. Clark, G. Danielson, A. Davies, P. Drossart, T. Encrenaz, F. Fanale, J. Granahan, G. Hansen, P. Herrera, C. Hibbitts, J. Hui, P. Irwin, T. Johnson, L. Kamp, H. Kieffer, F. Leader, E. Lellouch, R. Lopes-Gautier, D. Matson, T. McCord, R. Mehlman, A. Ocampo, G. Orton, M. Roos-Serote, M. Segura, J. Shirley, L. Soderblom, A. Stevenson, F. Taylor, J. Torson, A. Weir, and P. Weissman, Near-infrared spectroscopy and spectral mapping of Jupiter and the Galilean satellites: Results from *Galileo*'s initial orbit, *Science* **274**, 385–388, 1996.

Carlson, R., W. D. Smythe, R. M. C. Lopes-Gautier, A. G. Davies, L. W. Kamp, J. A. Mosher, L. A. Soderblom, F. E. Leader,

R. Mehlman, R. N. Clark, and F. P. Fanale, Distribution of sulfur dioxide and other infrared absorbers on the surface of Io, *Geophys. Res. Lett.* **24**, 2479–2482, 1997.

Carlson, R., M. S. Anderson, R. E. Johnson, W. D. Smythe, A. R. Hendrix, C. A. Barth, L. A. Soderblom, G. B. Hansen, T. B. McCord, J. B. Dalton, R. N. Clark, J. Shirley, A. Ocampo, and D. Matson, Hydrogen peroxide on the surface of Europa, *Science* **283**, 2062–2064, 1999a.

Carlson, R., R. E. Johnson, and M. S. Anderson, Sulfuric acid on Europa and the radiolytic sulfur cycle, *Science* **286**, 97–99, 1999b.

Carlson, R., M. S. Anderson, M. Wong, and R. E. Johnson, Radiolysis processes on Europa, *Geophys. Res. Abs.* **3**, 7457, 2001.

Carlson, R., M. S. Anderson, R. E. Johnson, M. B. Schulman, and A. H. Yavrouian, Sulfuric acid production on Europa: The radiolysis of sulfur in water ice, *Icarus* **157**, 456–463, 2002.

Carlson, R., M. S. Anderson, and R. E. Johnson, Radiolytic carbon compounds on Callisto, *Geophys. Res. Lett.* **submitted**, 2003a.

Carlson, R., M. S. Anderson, R. E. Johnson, R. Mehlman, J. H. Shirley, and J. A. Mosher, Distribution of hydrated sulfuric acid on Europa, *Icarus* **submitted**, 2003b.

Carr, M. H., M. J. S. Belton, C. R. Chapman, M. E. Davies, P. Geissler, R. Greenberg, A. S. McEwen, B. R. Tufts, R. Greeley, and R. Sullivan, Evidence for a subsurface ocean on Europa, *Nature* **391**, 363, 1998.

Casal, H. L. and J. C. Scaiano, Transient intermediates in the photochemistry of elemental sulfur in solution, *J. Photochem.* **30**, 253–257, 1985.

Chrisey, D. B., R. E. Johnson, J. W. Boring, and J. A. Phipps, Ejection of sodium from sodium sulfide by the sputtering of the surface of Io, *Icarus* **75**, 233–244, 1988a.

Chrisey, D. B., R. E. Johnson, J. W. Boring, and J. A. Phipps, Molecular ejection from low temperature sulfur by keV ions, *Surf. Sci.* **195**, 594–618, 1988b.

Chrisey, D. B., W. L. Brown, and J. W. Boring, Electronic excitation of condensed CO: Sputtering and chemical change, *Surf. Sci.* **225**, 130–140, 1990.

Chyba, C. F., Energy for microbial life on Europa, *Nature* **403**, 381–382, 2000.

Chyba, C. F. and K. P. Hand, Planetary science: Life without photosynthesis, *Science* **292**, 2026–2027, 2001.

Chyba, C. F. and C. B. Phillips, Possible ecosystems and the search for life on Europa, *Proc. Nat. Acad. Sci. USA* **98**, 801–804, 2001.

Clark, B. E. and R. E. Johnson, Interplanetary weathering: Surface erosion in outer space, *Eos* **77**, 141–145, 1996.

Cohen, C. M. S., E. C. Stone, and R. S. Selesnick, Energetic ion observations in the middle jovian magnetosphere, *J. Geophys. Res.* **106**, 29 871–29 882, 2001.

Cooper, C., C. Phillips, J. Green, X. Wu, R. Carlson, L. Tampari, R. Terrile, R. Johnson, J. Eraker, and N. Makris, Europa exploration: Science and mission priorities, in *The Future of Solar System Exploration 2003–2013*, M. Sykes (ed.), ASP, pp. 217–252, 2002.

Cooper, J. F., R. E. Johnson, B. H. Mauk, H. B. Garrett, and N. Gehrels, Energetic ion and electron irradiation of the icy Galilean satellites, *Icarus* **149**, 133–159, 2001.

Cooper, P. D., R. E. Johnson, and T. I. Quickenden, Hydrogen peroxide dimers and the production of O_2 in the surfaces of icy satellites, *Icarus* **166**, 444–446, 2003.

Dalton, J. B. and R. N. Clark, Analysis of the europan surface composition based on *Galileo* NIMS spectra, *BAAS* **31**, 0, 1999.

Dalton, J. B., R. Mogul, H. K. Kagawa, S. L. Chan, and C. Jamieson, Near-infrared detection of potential evidence for microscopic organisms on Europa, *Astrobiol. J.* **3**, 505–529, 2003.

Dalton, J. B. I., *Constraints on the Surface Composition of Jupiter's Moon Europa Based on Laboratory and Spacecraft Data*, Ph.D. thesis, University of Colorado, 2000.

Delitsky, M. L. and A. L. Lane, Chemical schemes for surface modification of icy satellites: A road map, *J. Geophys. Res.* **102**, 16 385–16 390, 1997.

Delitsky, M. L. and A. L. Lane, Ice chemistry on the Galilean satellites, *J. Geophys. Res.* **103**, 31 391–31 404, 1998.

DellaGuardia, R. and F. Johnston, Radiation-induced reaction of sulfur and water, *Radiat. Res.* **84**, 259–264, 1980.

Dominé, F. and P. B. Shepson, Air-snow interactions and atmospheric chemistry, *Science* **297**, 1506–1510, 2002.

Domingue, D. L. and A. Hendrix, Temporal variations in the surface chemistry of the icy Galilean satellites, *Icarus* **submitted**, 2003.

Domingue, D. L. and A. L. Lane, IUE views Europa: Temporal variations in the UV, *Geophys. Res. Lett.* **25**, 4421–4424, 1998a.

Domingue, D. L. and A. L. Lane, Secular ultraviolet studies of the Galilean satellites, in *Ultraviolet Astrophysics Beyond the IUE Final Archive*, p. 13, 1998b.

Domingue, D. L., A. Lane, and R. Beyer, IUE's detection of tenuous SO_2 frost on Ganymede and its rapid time variability, *Geophys. Res. Lett.* **25**, 3117–312–, 1998.

Donaldson, G. W. and F. J. Johnston, The radiolysis of colloidal sulfur, *J. Phys. Chem.* **72**, 3552–3558, 1968.

Donaldson, G. W. and F. J. Johnston, The radiolysis of colloidal sulfur: A mechanism for solubilization, *J. Phys. Chem.* **75**, 756–763, 1971.

Ehrenfreund, P., M. P. Bernstein, J. P. Dworkin, S. A. Sandford, and L. J. Allamandola, The photostability of amino acids in space, *ApJ* **550**, L95–L99, 2001.

Eviatar, A. and D. D. Barbosa, Jovian magnetospheric neutral wind and auroral precipitation flux, *J. Geophys. Res.* **89**, 7393–7398, 1984.

Fanale, F. P., T. V. Johnson, and D. L. Matson, Io: A surface evaporite deposit?, *Science* **186**, 922–925, 1974.

Fischer, H. M., E. Pehlke, G. Wibberbez, L. J. Lanzerotti, and J. D. Mihalov, High-energy charged particles in the innermost jovian magnetosphere, *Science* **272**, 856–858, 1996.

Geissler, P., C. Phillips, and T. Denk, The color of Europa: Comparisons with Ganymede, Callisto, and Antarctica, in *Workshop on Remote Sensing of Planetary Ices: Earth and Other Solid Bodies*, Flagstaff, 2000.

Gerakines, P. A. and M. H. Moore, Carbon suboxide in astrophysical ice analogs, *Icarus* **154**, 372–380, 2001.

Gerakines, P. A., W. A. Schutte, and P. Ehrenfreund, Ultraviolet processing of interstellar ice analogs: I. Pure ices, *A&A* **312**, 289–305, 1996.

Gerakines, P. A., M. H. Moore, and R. L. Hudson, Carbonic acid production in H_2O:CO_2 ices. UV photolysis *vs.* proton bombardment, *A&A* **357**, 793–800, 2000.

Gerakines, P. A., M. H. Moore, and R. L. Hudson, Energetic processing of laboratory ice analogs: UV photolysis versus ion bombardment, *J. Geophys. Res.* **106**, 33 381–33 386, 2001.

Gomis, O., M. A. Satorre, G. Leto, and G. Strazzulla, Hydrogen peroxide formation by ion implantation in water ice, *Planet. Space Sci.* **52**, 371–378, 2004.

Gradie, J., P. Thomas, and J. Veverka, The surface composition of Amalthea, *Icarus* **44**, 373–387, 1980.

Gromov, V. V. and L. G. Karaseva, Radiation defects in irradiated specimens of potasium sulfate, *High Energy Chem.* **1**, 45–50, 1967.

Gromov, V. V. and J. R. Morton, Paramagnetic centers in irradiated potassium sulfate, *Canadian J. Chemistry* **44**, 527–528, 1966.

Gromov, V. V. and V. I. Spitsyn, Radiochemical determination of the radiolysis products of barium, strontium, and calcium sulfates, *High Energy Chem.* **3**, 162–163, 1969.

Grundy, W. M., J. R. Spencer, and M. W. Buie, Thermal inertia of Europa's H_2O ice surface component, *BAAS* **33**, 0, 2001.

Hage, W., K. R. Liedl, A. Hallbrucker, and E. Mayer, Carbonic acid in the gas phase and its astrophysical relevance, *Science* **279**, 1332–1335, 1998.

Hall, D. T., D. F. Strobel, P. D. Feldman, M. A. McGrath, and H. A. Weaver, Detection of an oxygen atmosphere on Jupiter's moon Europa, *Nature* **373**, 677–679, 1995.

Hall, D. T., P. D. Feldman, M. A. McGrath, and D. F. Strobel, The far-ultraviolet oxygen airglow of Europa and Ganymede, *ApJ* **499**, 475–481, 1998.

Hamilton, D. C., G. Gloeckler, S. M. Krimigis, and L. J. Lanzerotti, Composition of nonthermal ions in the jovian magnetosphere, *J. Geophys. Res.* **86**, 8301–8318, 1981.

Hansen, G. B. and T. B. McCord, Amorphous and crystalline ice on the Galilean satellites: A balance between thermal and radiolytic processes, *J. Geophys. Res.*, **109**, 2149, 2004.

Hapke, B., On the sputter alteration of regoliths of outer solar system bodies, *Icarus* **66**, 270–279, 1986.

Hapke, B., Space weathering from Mercury to the asteroid belt, *J. Geophys. Res.* **106**, 10 039–10 074, 2001.

Hart, E. J. and R. L. Platzman, Radiation chemistry, in *Physical Mechanisms in Radiation Biology 1*, Erreva and M. A. Forssberg (eds), Academic Press, pp. 99–120, 1961.

Head, J. W. and R. T. Pappalardo, Brine mobilization during lithospheric heating on Europa: Implications for formation of chaos terrain, lenticula texture, and color variations, *J. Geophys. Res.* **104**, 27 143–27 155, 1999.

Hendrix, A. R., C. A. Barth, and C. W. Hord, Ganymede's ozone-like absorber: Observations by the *Galileo* ultraviolet spectrometer, *J. Geophys. Res.* **104**, 14 169–14 178, 1999a.

Hendrix, A. R., C. A. Barth, A. I. F. Stewart, C. W. Hord, and A. L. Lane, Hydrogen peroxide on the icy Galilean satellites, in *Lunar and Planetary Science Conference Abstracts*, p. 2043, 1999b.

Hendrix, A. R., R. W. Carlson, R. Mehlman, and W. D. Smythe, Europa as measured by *Galileo* NIMS and UVS (abstract), in *Jupiter after Galileo and Cassini*, Lisbon, p. 108, 2002.

Hibbitts, C. A., T. B. McCord, G. B. Hansen, and J. E. Klemaszewski, Possible exogenic and impact origins for carbon dioxide on the surface of Callisto, in *Lunar and Planetary Science Conference Abstracts*, p. 1540, 1999.

Hibbitts, C. A., T. B. McCord, and G. B. Hansen, Distributions of CO_2 and SO_2 on the surface of Callisto, *J. Geophys. Res.* **105**, 22 541–22 558, 2000.

Hillier, J., P. Helfenstein, and J. Veverka, Latitude variations of the polar caps on Ganymede, *Icarus* **124**, 308–317, 1996.

Huang, S. and E. R. Johnson, The radiation-induced decomposition of some inorganic sulfates, in *Effects of High Energy Radiation on Inorganic Substances*, Seattle, pp. 121–138, 1965.

Hudson, R. L. and M. H. Moore, Laboratory studies of the formation of methanol and other organic molecules by water+carbon monoxide radiolysis: Relevance to comets, icy satellites, and interstellar ices, *Icarus* **140**, 451–461, 1999.

Ikeya, M., H. Sasaoka, H. Toda, K. Kanosue, and M. Hirai, Future ESR and optical dating of outer planet icy materials, *Quatern. Sci. Rev.* **16**, 431–435, 1997.

Ip, W., A. Kopp, D. J. Williams, R. W. McEntire, and B. H. Mauk, Magnetospheric ion sputtering: The case of Europa and its surface age, *Adv. Space Res.* **26**, 1649–1652, 2000.

Ip, W.-H., D. J. Williams, R. W. McEntire, and B. Mauk, Energetic ion sputtering effects at Ganymede, *Geophys. Res. Lett.* **24**, 2631–2634, 1997.

Ip, W.-H., D. J. Williams, R. W. McEntire, and B. H. Mauk, Ion sputtering and surface erosion at Europa, *Geophys. Res. Lett.* **25**, 829–832, 1998.

Johnson, R. E., Polar frost formation on Ganymede, *Icarus* **62**, 344–347, 1985.

Johnson, R. E., Application of laboratory data to the sputtering of a planetary regolith, *Icarus* **78**, 206–210, 1989.

Johnson, R. E., *Energetic Charged-Particle Interactions with Atmospheres and Surfaces*, Springer-Verlag, 1990.

Johnson, R. E., Sputtering of ices in the outer solar system, *Rev. Mod. Phys.* **68**, 305–312, 1996.

Johnson, R. E., Polar "caps" on Ganymede and Io revisited, *Icarus* **128**, 469–471, 1997.

Johnson, R. E., Sputtering and desorption from icy surfaces, in *Solar System Ices*, ASSL, p. 303, 1998.

Johnson, R. E., Comment on "Laboratory studies of the optical properties and stability of oxygen on Ganymede" by Baragiola and Bahr, *J. Geophys. Res.* **104**, 14 179–14 182, 1999.

Johnson, R. E., Sodium at Europa, *Icarus* **143**, 429–433, 2000.

Johnson, R. E., Surface chemistry in the jovian magnetosphere radiation environment, in *Chemical Dynamics in Extreme Environments*, R. Dessler (ed.), Adv. Ser. in Phys. Chem., pp. 390–419, 2001.

Johnson, R. E. and W. A. Jesser, O_2/O_3 microatmospheres in the surface of Ganymede, *ApJ* **480**, L79–L82, 1997.

Johnson, R. E. and T. I. Quickenden, Photolysis and radiolysis of water ice on outer solar system bodies, *J. Geophys. Res.* **102**, 10 985–10 996, 1997.

Johnson, R. E., L. J. Lanzerotti, W. L. Brown, and T. P. Armstrong, Erosion of Galilean satellite surfaces by jovian magnetosphere particles, *Science* **212**, 1027–1030, 1981.

Johnson, R. E., L. J. Lanzerotti, and W. L. Brown, Planetary applications of ion induced erosion of condensed gas frosts, *Nucl. Inst. Meth. Phys. Res. A* **198**, 147–158, 1982.

Johnson, R. E., J. W. Boring, C. T. Reimann, L. A. Barton, J. W. Sieveka, J. W. Garrett, K. R. Farmer, W. L. Brown, and L. J. Lanzerotti, Plasma ion-induced molecular ejection on the Galilean satellites: Energies of ejected molecules, *Geophys. Res. Lett.* **10**, 892–895, 1983.

Johnson, R. E., M. L. Nelson, T. B. Nccord, and J. C. Gradie, Analysis of *Voyager* images of Europa: Plasma bombardment, *Icarus* **75**, 423–436, 1988.

Johnson, R. E., R. M. Killen, J. H. Waite, and W. S. Lewis, Europa's surface composition and sputter-produced ionosphere, *Geophys. Res. Lett.* **25**, 3257–3260, 1998.

Johnson, R. E., F. Leblanc, B. V. Yakshinskiy, and T. E. Madey, Energy distributions for desorption of sodium and potassium from ice: The Na/K ratio at Europa, *Icarus* **156**, 136–142, 2002.

Johnson, R. E., T. I. Quickenden, P. D. Cooper, A. J. McKinley, and C. Freeman, The production of oxidants in Europa's surface, *Astrobiol.* **3**, 823–850, 2003.

Jurac, S., R. A. Baragiola, R. E. Johnson, and E. C. Sittler, Charging of ice grains by low-energy plasmas: Application to Saturn's E ring, *J. Geophys. Res.* **100**, 14 821–14 832, 1995.

Jurac, S., R. E. Johnson, and J. D. Richardson, Saturn's E Ring and production of the neutral torus, *Icarus* **149**, 384–396, 2001.

Karaseva, L. G., L. T. Zhuravlev, V. V. Gromov, and V. I. Spitsyn, A mass spectrometric study of the thermal decomposition products of gamma-irradiated strontium sulfate, *High Energy Chem.* **2**, 483–486, 1968.

Karaseva, L. G., V. V. Gromov, and L. I. Stepovaya, Kinetics of the accumulation of radiation defects in anhydrous beryllium sulfate and its crystalline hydrates, *High Energy Chem.* **7**, 152–153, 1973.

Kargel, J. S., Brine volcanism and the interior structures of asteroids and icy satellites, *Icarus* **94**, 368–390, 1991.

Kargel, J. S., J. Z. Kaye, J. W. Head, G. M. Marion, R. Sassen, J. K. Crowley, O. P. Ballesteros, S. A. Grant, and D. L. Hogenboom, Europa's crust and ocean: Origin, composition, and the prospects for life, *Icarus* **148**, 226–265, 2000.

Kargel, J. S., J. W. Head, D. L. Hogenboom, K. K. Khurana, and G. Marion, The system sulfuric acid-magnesium sulfate-water: Europa's ocean properties related to thermal state, in *Lunar and Planetary Science Conference Abstracts*, p. 2138, 2001.

Khanna, R. K., J. C. Pearl, and R. Dahmani, Infrared spectra and structure of solid phases of sulfur trioxide: Possible identification of solid SO_3 on Io's surface, *Icarus* **115**, 250–257, 1995.

Khriachtchev, L., M. Pettersson, S. Tuominen, and M. Räsänen, Photochemistry of hydrogen peroxide in solid argon, *J. Chem. Phys.* **107**, 7252–7259, 1997.

Khriachtchev, L., M. Pettersson, S. Jolkkonen, S. Pehkonen, and M. Räsänen, Photochemistry of hydrogen peroxide in Kr and Xe matrixes, *J. Chem. Phys.* **112**, 2187–2194, 2000.

Khurana, K. K., M. Kivelson, D. Stevenson, G. Schubert, C. Russell, R. Walker, and C. Polanskey, Induced magnetic fields as evidence for subsurface oceans in Europa and Callisto, *Nature* **395**, 777–780, 1998.

Kimmel, G. A. and T. M. Orlando, Low-energy (5–120 eV) electron-stimulated dissociation of amorphous D_2O Ice: $D(^2S)$, $O(^3P_{2,1,0})$, and $O(^1D_2)$ yields and velocity distributions, *Phys. Rev. Lett.* **75**, 2606–2609, 1995.

Kimmel, G. A., T. M. Orlando, C. Vézina, and L. Sanche, Low-energy electron-stimulated production of molecular hydrogen from amorphous water ice, *J. Chem. Phys.* **101**, 3282–3286, 1994.

Kivelson, M. G., K. K. Khurana, D. J. Stevenson, L. Bennett, S. Joy, C. T. Russell, R. J. Walker, C. Zimmer, and C. Polanskey, Europa and Callisto: Induced or intrinsic fields in a periodically varying plasma environment, *J. Geophys. Res.* **104**, 4609–4626, 1999.

Kliore, A. J., D. P. Hinson, F. M. Flasar, A. F. Nagy, and T. E. Cravens, The ionosphere of Europa from *Galileo* radio occultations, *Science* **277**, 355–358, 1997.

Kliore, A. J., A. Anabtawi, and A. F. Nagy, The ionospheres of Europa, Ganymede, and Callisto, in *Eos*, vol. 82, pp. P12B–0506, 2001.

Kliore, A. J., A. Anabtawi, R. G. Herrera, S. W. Asmar, A. F. Nagy, D. P. Hinson, and F. M. Flasar, Ionosphere of Callisto from *Galileo* radio occultation observations, *J. Geophys. Res.* **107**, 1407, 2002.

Krüger, H., A. V. Krivov, and E. Grün, A dust cloud of Ganymede maintained by hypervelocity impacts of interplanetary micrometeoroids, *Planet. Space Sci.* **48**, 1457–1471, 2000.

Krylova, Z. L. and P. I. Dolin, Radiolysis of water adsorbed on silica-gel, in *Second Tihany Symposium on Radiation Chemistry*, J. Dobo and P. Hedvig (eds), Akademiai Kaido, Budapest, pp. 133–138, 1967.

Küppers, H. and N. M. Schneider, Discovery of chlorine in the Io torus, *Geophys. Res. Lett.* **27**, 513–516, 2000.

Lane, A. L., R. M. Nelson, and D. L. Matson, Evidence for sulphur implantation in Europa's UV absorption band, *Nature* **292**, 38–39, 1981.

Langford, V. S., J. M. Allan, and T. I. Quickenden, Identification of H_2O–HO in argon matrices, *J. Am. Chem. Soc.* **122**, 12 859–12 863, 2000.

Lanzerotti, L. J., W. L. Brown, J. M. Poate, and W. M. Augustyniak, On the contribution of water products from Galilean satellites to the jovian magnetosphere, *Geophys. Res. Lett.* **5**, 155–158, 1978.

Lanzerotti, L. J., W. L. Brown, W. M. Augustyniak, R. E. Johnson, and T. P. Armstrong, Laboratory studies of charged particle erosion of SO_2 ice and applications to the frosts of Io, *ApJ* **259**, 920–929, 1982.

Lanzerotti, L. J., W. L. Brown, and K. J. Marcantonio, Experimental study of erosion of methane ice by energetic ions and some considerations for astrophysics, *ApJ* **313**, 910–919, 1987.

Leblanc, F., R. E. Johnson, and M. E. Brown, Europa's sodium atmosphere: An ocean source?, *Icarus* **159**, 132–144, 2002.

Lellouch, E., G. Paubert, J. I. Moses, N. M. Schneider, and D. F. Strobel, Volcanically emitted sodium chloride as a source for Io's neutral clouds and plasma torus, *Nature* **421**, 45–47, 2003.

Leto, G. and G. A. Baratta, Ly-alpha photon induced amorphization of Ic water ice at 16 Kelvin. Effects and quantitative comparison with ion irradiation, *A&A* **397**, 7–13, 2003.

Li, Y.-H., *A Compendium of Geochemistry*, Princeton University Press, 2000.

Liu, Y., A. F. Nagy, K. Kabin, M. R. Combi, D. L. Dezeeuw, T. I. Gombosi, and K. G. Powell, Two-species, 3D, MHD simulation of Europa's interaction with Jupiter's magnetosphere, *Geophys. Res. Lett.* **27**, 1791–1794, 2000.

Livingston, F. E., J. A. Smith, and S. M. George, General trends for bulk diffusion in ice and surface diffusion on ice, *J. Phys. Chem. A* **106**, 6309–6318, 2002.

Lovelock, J., *The Ages of Gaia: A Biography of our Living Earth*, Bantain Books, 1988.

Madey, T. E., R. E. Johnson, and T. M. Orlando, Far-out surface science: Radiation-induced surface processes in the solar system, *Surface Science* **500**, 838–858, 2002.

Marion, G. M., A molal-based model for strong acid chemistry at low temperatures (< 200 to 298 K), *Geochem. Cosmochem. Acta* **67**, 1755, 2003.

Matich, A. J., M. G. Bakker, D. Lennon, T. Quickenden, and C. Freeman, O_2 luminescence from UV-excited H_2O and D_2O ices, *J. Phys. Chem.* **97**, 10 539–10 553, 1993.

Matson, D. L., T. V. Johnson, and F. P. Fanale, Sodium D-Line emission from Io: Sputtering and resonant scattering hypothesis, *ApJ* **192**, L43–L46, 1974.

Mauk, B. H., S. A. Gary, M. Kane, E. P. Keath, S. M. Krimigis, and T. P. Armstrong, Hot plasma parameters of Jupiter's inner magnetosphere, *J. Geophys. Res.* **101**, 7685–7696, 1996.

Mauk, B. H., R. W. McEntire, D. J. Williams, A. Lagg, E. C. Roelof, S. M. Krimigis, T. P. Armstrong, T. A. Fritz, L. J. Lanzerotti, J. G. Roederer, and B. Wilken, *Galileo*-measured depletion of near-Io hot ring current plasmas since the *Voyager* epoch, *J. Geophys. Res.* **103**, 4715–4722, 1998.

Mauk, B. H., D. G. Mitchell, S. M. Krimigis, E. C. Roelof, and C. P. Paranicas, Energetic neutral atoms from a trans-Europa gas torus at Jupiter, *Nature* **421**, 920–922, 2003.

McCord, T. B., R. Carlson, W. Smythe, G. Hansen, R. Clark, C. Hibbitts, F. Fanale, J. Granahan, M. Segura, D. Matson, T. Johnson, and P. Martin, Organics and other molecules in the surfaces of Callisto and Ganymede, *Science* **278**, 271–275, 1997.

McCord, T. B., G. B. Hansen, R. N. Clark, P. D. Martin, C. A. Hibbitts, F. P. Fanale, J. C. Granahan, M. Segura, D. L. Matson, T. V. Johnson, R. W. Carlson, W. D. Smythe, and G. E. Danielson, Non-water-ice constituents in the surface material of the icy Galilean satellites from the *Galileo* Near Infrared Mapping Spectrometer investigation, *J. Geophys. Res.* **103**, 8603–8626, 1998a.

McCord, T. B., G. B. Hansen, F. P. Fanale, R. W. Carlson, D. L. Matson, T. V. Johnson, W. D. Smythe, J. K. Crowley, P. D. Martin, A. Ocampo, C. A. Hibbitts, and J. C. Granahan, Salts on Europa's surface detected by *Galileo*'s Near Infrared Mapping Spectrometer, *Science* **280**, 1242–1245, 1998b.

McCord, T. B., G. B. Hansen, D. L. Matson, T. V. Jonhson, J. K. Crowley, F. P. Fanale, R. W. Carlson, W. D. Smythe, P. D.

Martin, C. A. Hibbitts, J. C. Granahan, and A. Ocampo, Hydrated salt minerals on Europa's surface from the *Galileo* Near Infrared Mapping Spectrometer (NIMS) investigation, *J. Geophys. Res.* **104**, 11 827–11 852, 1999.

McCord, T. B., G. B. Hansen, and C. A. Hibbitts, Hydrated salt minerals on Ganymede's surface: Evidence of an ocean below, *Science* **292**, 1523–1525, 2001a.

McCord, T. B., T. M. Orlando, G. Teeter, G. B. Hansen, M. T. Sieger, N. G. Petrik, and L. van Keulen, Thermal and radiation stability of the hydrated salt minerals epsomite, mirabilite, and natron under Europa environmental conditions, *J. Geophys. Res.* **106**, 3311–3320, 2001b.

McCord, T. B., G. Teeter, G. B. Hansen, M. T. Sieger, and T. M. Orlando, Brines exposed to Europa surface conditions, *J. Geophys. Res.* **107**, 1029, 2002.

McEwen, A. S., Exogenic and endogenic albedo and color patterns on Europa, *J. Geophys. Res.* **91**, 8077–8097, 1986.

McGrath, M., Hubble Space Telescope observations of Europa and Ganymede, *Eos* pp. P52C–05, 2002.

McGrath, M. A., P. D. Feldman, D. F. Strobel, K. Retherford, B. Wolven, and H. W. Moos, HST/STIS ultraviolet imaging of Europa, *BAAS* **32**, 0, 2000.

McKinnon, W., Sulphate content of Europa's ocean and shell: Geological and astrobiological implications, *BAAS* **34**, 914–915, 2002.

McKinnon, W. B. and M. E. Zolensky, Sulphate content of Europa's ocean and shell, *Astrobiology*, **4**, 879–898, 2003.

Meier, R., B. A. Smith, T. C. Owen, E. E. Becklin, and R. J. Terrile, Near infrared photometry of the jovian ring and Adrastea, *Icarus* **141**, 253–262, 1999.

Mihalov, J. D., H. M. Fischer, E. Pehlke, and L. J. Lanzerotti, Energetic trapped electron measurements from the *Galileo* Jupiter probe, *Geophys. Res. Lett.* **27**, 2445–2448, 2000.

Mogro-Campero, A., Absorption of radiation belt particles by the inner satellites of Jupiter, in *Jupiter*, T. Gehrels (ed), University of Arizona Press, pp. 1190–1214, 1976.

Moore, J. M., E. Asphaug, D. Morrison, J. R. Spencer, C. R. Chapman, B. Bierhaus, R. J. Sullivan, F. C. Chuang, J. E. Klemaszewski, R. Greeley, K. C. Bender, P. E. Geissler, P. Helfenstein, and C. B. Pilcher, Mass movement and landform degradation on the icy Galilean satellites: Results of the *Galileo* nominal mission, *Icarus* **140**, 294–312, 1999.

Moore, M. H., Studies of proton-irradiated SO_2 at low temperatures: Implications for Io, *Icarus* **59**, 114–128, 1984.

Moore, M. H. and R. L. Hudson, Far-infrared spectra of cosmic-type pure and mixed ices, *A&AS* **103**, 45–56, 1994.

Moore, M. H. and R. L. Hudson, IR detection of H_2O_2 at 80 K in ion-irradiated laboratory ices relevant to Europa, *Icarus* **145**, 282–288, 2000.

Moore, M. H. and R. K. Khanna, Infrared and mass spectral studies of proton irradiated $H_2O + CO_2$ ice: Evidence for carbonic acid, *Spectrochim. Acta* **47**, 255–262, 1991.

Moore, M. H., R. Khanna, and B. Donn, Studies of proton irradiated $H_2O + CO_2$ and $H_2O + CO$ ices and analysis of synthesized molecules, *J. Geophys. Res.* **96**, 17 541–17 545, 1991.

Moore, M. H., R. L. Hudson, and R. W. Carlson, IR spectra of ion-irradiated ices containing SO_2 and H_2S, *BAAS* **34**, 902, 2002.

Moorthy, P. N. and J. J. Weiss, Radiation-induced formation of the univalent Mg^+, Zn^+, and Cd^+ from the divalent cations in g-irradiated ice, *Nature* **201**, 1317–1318, 1964.

Morris, R. V., In situ reworking (gardening) of the lunar surface: Evidence from the *Apollo* cores, in *Lunar and Planetary Science Conference*, pp. 1801–1811, 1978.

Morrison, D., ed., *Satellites of Jupiter*, 1982.

Nash, D. B. and F. P. Fanale, Io's surface composition based on reflectance spectra of sulfur/salt mixtures and proton-irradiation experiments, *Icarus* **31**, 40–80, 1977.

Nelson, R. M. and B. Betts, Laboratory infrared spectra (2.3–23 microns) of SO_2 phases: Applications to Io surface analysis, *Icarus* **117**, 402–419, 1995.

Nelson, R. M., A. L. Lane, D. L. Matson, G. J. Veeder, B. J. Buratti, E. F. Tedesco, Spectral geometric albedos of the Galilean satellites from 0.24 to 0.34 microns, *Icarus*, **72**, 358–380, 1987.

Nelson, R. M., W. D. Smythe, B. W. Hapke, and A. J. Cohen, On the effect of X-rays on the color of elemental sulfur: Implications for Jupiter's satellite Io, *Icarus* **85**, 326–334, 1990.

Neubauer, F. M., The sub-Alfvénic interaction of the Galilean satellites with the jovian magnetosphere, *J. Geophys. Res.* **103**, 19 843–19 866, 1998.

Nishijima, C., N. Kanamuru, and K. Titmura, Primary photochemical processes of sulfur in solution, *Bull. Chem. Soc. Japan* **49**, 1151–1152, 1976.

Noll, K. S., H. A. Weaver, and A. M. Gonnella, The albedo spectrum of Europa from 2200 Å to 3300 Å, *J. Geophys. Res.* **100**, 19 057–19 060, 1995.

Noll, K. S., R. E. Johnson, A. L. Lane, D. L. Domingue, and H. A. Weaver, Detection of ozone on Ganymede, *Science* **273**, 341–343, 1996.

Novak, A., Hydrogen bonding in solids. Correlation of spectroscopic and crystallographic data, *Structure and Bonding* **18**, 177–216, 1974.

Nyquist, R., C. Putzig, and M. Leugers, *Infrared and Raman Spectral Atlas of Inorganic Compounds and Organic Salts*, Academic Press, 1997.

Orlando, T. M. and G. A. Kimmel, The role of excitons and substrate temperature in low-energy (5–50 eV) electron-stimulated dissociation of amorphous D_2O ice, *Surf. Sci.* **390**, 79–85, 1997.

Pappalardo, R. T., K. K. Khurana, T. Denk, W. Ip, T. Rosanova, A. S. McEwen, T. V. Johnson, P. E. Helfenstein, J. W. Head, R. Goyal, J. Warnecke, M. G. Kivelson, G. Neukum, L. Gaddis, T. Becker, *Galileo* Imaging Team, and *Galileo* Magnetometer Team, A comparison of the plasma bombardment boundary on Ganymede's surface to *Galileo* imaging data, *BAAS* **30**, 1120, 1998.

Paranicas, C., W. R. Paterson, A. F. Cheng, B. H. Mauk, R. W. McEntire, L. A. Frank, and D. J. Williams, Energetic particle observations near Ganymede, *J. Geophys. Res.* **104**, 17 459–17 470, 1999.

Paranicas, C., R. W. Carlson, and R. E. Johnson, Electron bombardment of Europa, *Geophys. Res. Lett.* **28**, 673–676, 2001.

Paranicas, C., J. M. Ratliff, B. H. Mauk, C. Cohen, and R. E. Johnson, The ion environment near Europa and its role in surface energetics, *Geophys. Res. Lett.* **29**, 1074, 2002.

Pascu, D., S. P. Panossian, R. E. Schmidt, P. K. Seidelmann, and J. L. Hershey, B, V photometry of Thebe (JXIV), *Icarus* **98**, 38–42, 1992.

Pierazzo, E. and C. F. Chyba, Cometary delivery of biogenic elements to Europa, *Icarus* **157**, 120–127, 2002.

Pirronello, V., W. L. Brown, L. J. Lanzerotti, K. J. Marcantonio, and E. H. Simmons, Formaldehyde formation in a H_2O/CO_2 ice mixture under irradiation by fast ions, *ApJ* **262**, 636–640, 1982.

Pospieszalska, M. K. and R. E. Johnson, Magnetospheric ion bombardment profiles of satellites: Europa and Dione, *Icarus* **78**, 1–13, 1989.

Purves, N. G. and C. B. Pilcher, Thermal migration of water on the Galilean satellites, *Icarus* **43**, 51–55, 1980.

Reimann, C. T., J. W. Boring, R. E. Johnson, L. W. Garrett, and K. R. Farmer, Ion-induced molecular ejection from D_2O ice, *Applied Surface Science* **147**, 227–240, 1984.

Reynolds, R. T., S. W. Squyres, D. S. Colburn, and C. P. McKay, On the habitability of Europa, *Icarus* **56**, 246–254, 1983.

Rothschild, W. G., γ-ray decomposition of pure liquid sulfur dioxide, *J. Am. Chem. Soc.* **86**, 1307–1309, 1964.

Roush, T. L., Physical state of ices in the outer solar system, *J. Geophys. Res.* **106**, 33 315–33 324, 2001.

Sack, N. J., R. E. Johnson, J. W. Boring, and R. A. Baragiola, The effect of magnetospheric ion bombardment on the reflectance of Europa's surface, *Icarus* **100**, 534–540, 1992.

Sasaki, T., R. S. Williams, J. S. Wong, and D. A. Shirley, Radiation damage studies by x-ray photoelectron spectroscopy: I. Electron irradiated $LiNO_3$ and Li_2SO_4, *J. Chem. Phys.* **68**, 2718–2724, 1978.

Saur, J., D. F. Strobel, and F. M. Neubauer, Interaction of the jovian magnetosphere with Europa: Constraints on the neutral atmosphere, *J. Geophys. Res.* **103**, 19 947–19 962, 1998.

Schmitt, B., S. Rodriguez, and NIMS/*Galileo* Team, Cl_2SO_2 deposits near the Marduk's volcanic center on Io, *BAAS* **33**, 0, 2001.

Schou, J., O. Ellegaard, and B. H. Sorenson, Electronic sputtering of CO, in *Desorption Induced by Electronic Transitions DIET II*, W. Brenning and D. Menzel (eds), Springer, pp. 170–173, 1985.

Schreier, R., A. Eviatar, V. M. Vasyliunas, and J. D. Richardson, Modeling the Europa plasma torus, *J. Geophys. Res.* **98**, 21 231–21 243, 1993.

Schriver-Mazzuoli, L., A. Schriver, and H. Chaabount, Photooxidation of SO_2 and of SO_2 trapped in amorphous water ice studied by IR spectroscopy. Implications for Jupiter's satellite Europa, *Can. J. Phys.* **81**, 301–309, 2003.

Schulz, M., Jupiter's radiation belts, *Space Sci. Rev.* **23**, 277–318, 1979.

Shematovich, V. I. and R. E. Johnson, Near-surface oxygen atmosphere at Europa, *Adv. Space Res.* **27**, 1881–1888, 2001.

Shematovich, V. I., J. F. Cooper, and R. E. Johnson, Surface-bounded atmosphere of Europa, in *Eos*, pp. EAE03–A–13 094, 2003.

Shematovich, V. I., R. E. Johnson, J. F. Cooper, and M. C. Wong, Surface-bounded atmosphere of Europa, *Icarus*, **in press**, 2004.

Shi, M., R. A. Baragiola, D. E. Grosjean, R. E. Johnson, S. Jurac, and J. Schou, Sputtering of water ice surfaces and the production of extended neutral atmospheres, *J. Geophys. Res.* **100**, 26 387–26 396, 1995.

Shirley, J. H., R. W. Carlson, and M. S. Anderson, Upper limits for sodium and magnesium hydroxides on Europa (abstract), *Eos* **80**, F604, 1999.

Shoemaker, E. M., B. K. Lucchitta, D. E. Wilhelms, J. B. Plescia, and S. W. Squyres, The geology of Ganymede, in *Satellites of Jupiter*, D. Morrison (ed), University of Arizona Press, pp. 435–520, 1982.

Sieger, M. T., W. C. Simpson, and T. M. Orlando, Production of O_2 on icy satellites by electronic excitation of low-temperature water ice, *Nature* **394**, 554–556, 1998.

Sieveka, E. M. and R. E. Johnson, Thermal- and plasma-induced molecular redistribution on the icy satellites, *Icarus* **51**, 528–548, 1982.

Sieveka, E. M. and R. E. Johnson, Nonisotropic coronal atmosphere on Io, *J. Geophys. Res.* **90**, 5327–5331, 1985.

Simonelli, D. P., L. Rossier, P. C. Thomas, J. Veverka, J. A. Burns, and M. J. S. Belton, Leading/trailing albedo asymmetries of Thebe, Amalthea, and Metis, *Icarus* **147**, 353–365, 2000.

Simpson, J. A., D. Hamilton, G. Lentz, R. B. McKibben, A. Mogro-Campero, M. Perkins, K. R. Pyle, A. J. Tuzzolino, and J. J. O'Gallagher, Protons and electrons in Jupiter's magnetic field: Results from the University of Chicago experiment on *Pioneer 10*, *Science* **183**, 306–309, 1974.

Skuja, L., M. Hirano, and H. Hosono, Oxygen-related intrinsic defects in glassy SiO_2: Interstitial ozone molecules, *Phys. Rev. Lett.* **84**, 302–305, 2000.

Smith, R. S. and B. D. Kay, Adsorption, desorption, and crystallization kinetics in nanoscale water films, *Recent Res. Devel. Phys. Chem.* **1**, 209–219, 1997.

Spencer, J. R. and W. M. Calvin, Condensed O_2 on Europa and Callisto, *AJ* **124**, 3400–3403, 2002.

Spencer, J. R. and A. Klesman, New observations of molecular oxygen on Europa and Ganymede, *BAAS* **33**, 0, 2001.

Spencer, J. R., W. M. Calvin, and M. J. Person, CCD spectra of the Galilean satellites: Molecular oxygen on Ganymede, *J. Geophys. Res.* **100**, 19 049–19 056, 1995.

Spencer, J. R., L. K. Tamppari, T. Z. Martin, and L. D. Travis, Temperatures on Europa from *Galileo* PPR: Nighttime thermal anomalies, *Science* **284**, 1514–1516, 1999.

Spinks, J. W. T. and R. J. Woods, *An Introduction to Radiation Chemistry*, Wiley, 1990.

Spitsyn, V. I., V. V. Gromov, and L. G. Karaseva, EPR spectra of radioactive and irradiated samples of calcium, strontium, and barium sulfates, *Doklady Phys. Chem.* (translation) **159**, 1017–1020, 1964.

Squyres, S. W., R. T. Reynolds, and P. M. Cassen, Liquid water and active resurfacing on Europa, *Nature* **301**, 225, 1983.

Steudel, R., G. Holdt, and A. T. Young, On the colors of Jupiter's satellite Io: Irradiation of solid sulfur at 77 K, *J. Geophys. Res.* **91**, 4971–4977, 1986.

Stevenson, D. J., Volcanism and igneous processes in small icy satellites, *Nature* **298**, 142–144, 1982.

Stirniman, M. J., C. Huang, R. S. Smith, S. A. Joyce, and B. D. Kay, The adsorption and desorption of water on single crystal MgO(100): The role of surface defects, *J. Chem. Phys.* **105**, 1295–1298, 1996.

Strazzulla, G., Chemistry of ice induced by bombardment with energetic charged particles, in *Solar System Ices*, pp. 281–302, 1998.

Strazzulla, G., G. Leto, O. Gomis, and M. A. Satorre, Implantation of carbon and nitrogen ions in water ice, *Icarus* **164**, 163–169, 2003.

Taub, I. A. and K. Eiben, Transient solvated electron, hydroxyl, and hydroperoxy radicals in pulse-irradiated crystalline ice, *J. Chem. Phys.* **49**, 2499–2513, 1968.

Thorne, R. M., D. J. Williams, L. D. Zhang, and S. Stone, Energetic electron butterfly distributions near Io, *J. Geophys. Res.* **104**, 14 755–14 766, 1999.

Tiscareno, M. S. and P. E. Geissler, Can re-distributed material by sputtering explain the hemispheric dichotomy of Europa?, *Icarus* **161**, 90–101, 2003.

Torrisi, L., S. Coffa, G. Foti, R. E. Johnson, D. B. Chrisey, and J. W. Boring, Threshold dependence in the electronic sputtering of condensed sulfur, *Phys. Rev. B* **38**, 1516–1519, 1988.

Vidal, R. A., D. Bahr, R. A. Baragiola, and M. Peters, Oxygen on Ganymede: Laboratory studies, *Science* **276**, 1839–1842, 1997.

Volwerk, M., M. G. Kivelson, K. K. Khurana, and R. L. McPherron, Probing Ganymede's magnetosphere with field line resonances, *J. Geophys. Res.* **104**, 14 729–14 738, 1999.

Walters, M. D., J. W. Boring, R. Johnson, and W. Jesser, Crystallization of SiO by He^+ bombardment, *Radiation Effects and Defects in Solids* **106**, 189–201, 1988.

Watanabe, N., T. Horii, and A. Kouchi, Measurements of D_2 yields from amorphous D_2O ice by ultraviolet irradiation at 12 K, *ApJ* **541**, 772–778, 2000.

Wiens, R. C., D. S. Burnett, W. F. Calaway, C. S. Hansen, K. R. Lykke, and M. J. Pellin, Sputtering products of sodium sulfate: Implications for Io's surface and for sodium-bearing molecules in the Io torus, *Icarus* **128**, 386–397, 1997.

Williams, D. J., B. Mauk, and R. W. McEntire, Properties of Ganymede's magnetosphere as revealed by energetic particle observations, *J. Geophys. Res.* **103**, 17 523–17 534, 1998.

Wong, M. C. and R. E. Johnson, A three-dimensional azimuthally symmetric model atmosphere for Io: 2. Plasma effect on the surface, *J. Geophys. Res.* **101**, 23 255–23 260, 1996.

Wong, M. C. and W. H. Smyth, Model calculations for Io's atmosphere at eastern and western elongations, *Icarus* **146**, 60–74, 2000.

Wong, M. C., R. W. Carlson, J. F. Cooper, and R. E. Johnson, Model calculations for the icy Galilean satellite atmospheres, *Icarus* **to be submitted**, 2004.

Wourtzel, E., Actions chimiques du rayonnement a, *J. Phys. Radium* **1**, 77–96, 1920.

Yakshinskiy, B. V. and T. E. Madey, Photon-stimulated desorption as a substantial source of sodium in the lunar atmosphere, *Nature* **400**, 642–644, 1999.

Yakshinskiy, B. V. and T. E. Madey, Electron- and photon-stimulated desorption of K from ice surfaces, *J. Geophys. Res.* **106**, 33 303–33 308, 2001.

Zahnle, K., L. Dones, and H. F. Levison, Cratering rates on the Galilean satellites, *Icarus* **136**, 202–222, 1998.

Zeleznik, F. J., Thermodynamic properties of the aqueous sulfuric acid system to 350 K, *J. Phys. Chem. Ref. Data* **20**, 1157–1200, 1991.

Zolotov, M. Y. and E. L. Shock, Composition and stability of salts on the surface of Europa and their oceanic origin, *J. Geophys. Res.* **106**, 32 815–32 828, 2001.